The structure under the Warramunga seismic array: a study of Rayleigh wave near surface dispersion

Michael H. Worthington

THE STRUCTURE UNDER THE WARRAMUNGA SEISMIC ARRAY : A STUDY OF RAYLEIGH WAVE NEAR SURFACE DISPERSION

BY

MICHAEL H. WORTHINGTON

A thesis submitted for the degree of Master of Science in the University of Durham

Hatfield College

September 1969

CONTENTS

SUMMARY

A model of the structure under the Warramunga Seismic array, in Northern Australia, was deduced from a study of the surface wave dispersion. The waves had periods of a quarter to one and a half seconds and originated from mine blasts approximately thirty kilometres from the array. The dominant mode observed was tentatively assumed to be the first higher Rayleigh mode.

Dispersion curves were obtained using a number of techniques and a layered structure, dipping to the south-east was postulated. There was also evidence of a complex structure in the region of the cross-over point. Both these conclusions are in agreement with previous work.

INTRODUCTION

In this study, an attempt was made to deduce a structure beneath a seismic array by observing the dispersion of surface waves. The signals originated from mine-blasting some twenty to thirty kilometres distant from the array, and the periods of the waves were between a quarter and one and a half seconds.

The Warramunga seismic array is situated in the centre of the Northern Territories, Australia, forty-five kilometres south-east of the mining town, Tennant Creek. It consists of twenty Willmore Mark II seismometers, arranged in two arms at right angles. The arms are approximately twenty-two kilometres long. The structure beneath the array is believed to be complex.

Although the aim of the experiment was to improve on existing structural models, it was more a test of the potentiality of surface wave analysis, since the adequacy of this technique applied to complex near surface structures is not proven.

CHAPTER I

I1 PREVIOUS WORK

Detailed analysis of teleseismic signals requires a correction to be applied to arrival times, which is a function of the crustal structure beneath the array. Ideally, one hopes to be able to assume a homogeneous and symmetrical model. This is far from the case at Warramunga.

A 'residual' is the difference between a theoretical arrival time for an event (calculated from the standard Jeffrey-Bullen tables) and the actual arrival time. The trend of residuals across the Warramunga array are found to be in the same direction for events located at opposite azimuths. This suggests that the deviations are due to the structure beneath the array and not to errors in the Jeffrey-Bullen tables.

Cleary, Wright and Muirhead (1968) studied signals from an event in South Africa and an event in the Aleutian Islands and used equations developed by Niazi (1966) to calculate a dipping structure from residuals. They concluded that a layer dipping at 6.5 degrees in a direction of 235 degrees gave the best fit to the data. They also suggested that particularly anomalous results for pits B1, B2 and R1 were due to a dipping interface rising abruptly in the vicinity of the array cross-over point.

Underwood et al (1967) let off a timed explosion near the end of the Blue line (see Figure 4) and observed refracted P arrivals at the pits. He concluded that an interface, 0.99 kilometres below the shot, dipped at 5.3 degrees in a direction of 205.5 degrees and separated strata of 5.42 and 6.10 kilometres per second. However, it is likely that a model involving

a single dipping interface is too simple, because good agreement was never obtained between models from residual calculations and Underwood's data.

Corbishley (PhD thesis 1969) studied a large number of events from all azimuths and deduced a model where the dip of the layer varied from pit to pit. Two events from exactly opposite azimuths should be effected similarly by the structure under the array but will not be if a dipping layer exists. However, if the azimuth is varied until the ray paths are at right angles to the dip, the difference in residuals of the two events will be zero. Corbishley plotted delay time (e.g. residual) against azimuth for each seismometer and fitted a sine curve to the data.

$$\text{Delay Time } t = A + B\sin(\text{Azimuth} + \phi)$$

where ϕ = a phase term.

Since $\sin(AZ + \phi)$ is a maximum when $AZ = 90^\circ - \phi$ and t is a maximum when the azimuth is in the direction of the dip, Corbishley was able to deduce a residual for each pit and the variation of dip over the area. See Figures 1 and 2. Figure 2 supports a suggestion by Muirhead that the structure under the red arm is more complex than under the blue.

Although Figure 1 is an improvement on previous models, it still only represents a rough approximation to the actual structure. Corbishley obtained a better fit by imposing a double sine curve on his data. This could be interpreted as evidence for a double layer. However, the ideal fit would be a curve with a very complex mathematical expression and the physical significance is completely lost. Kelly [Personal

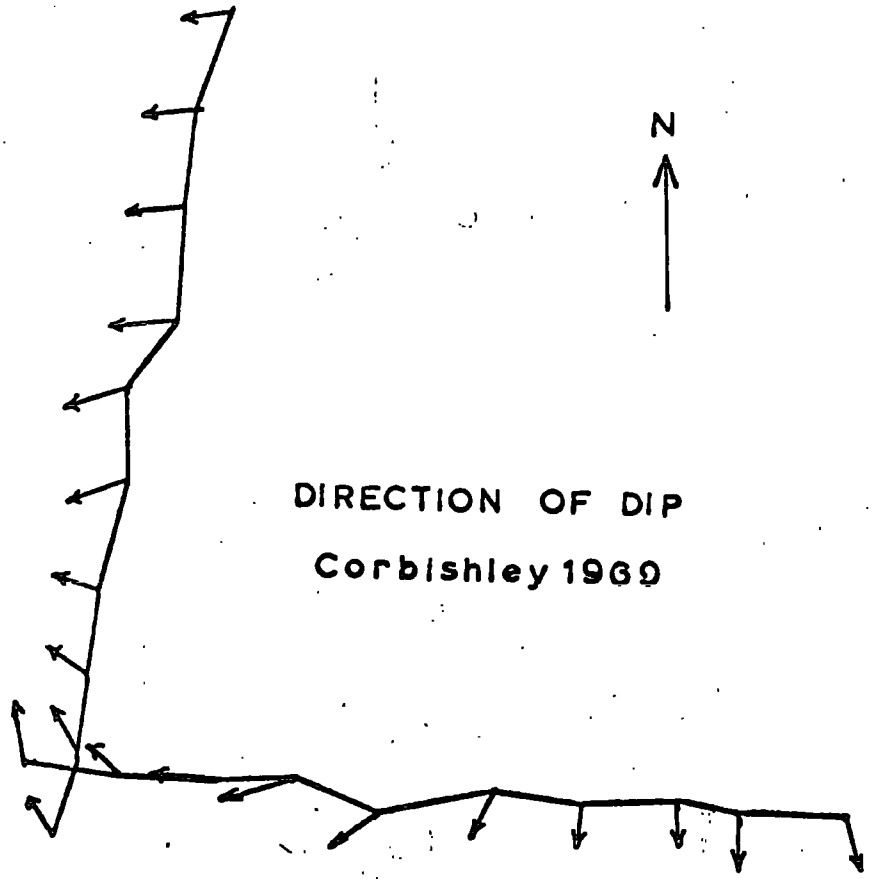
N
DIRECTION OF DIP
Corbishley 1969

FIG 1

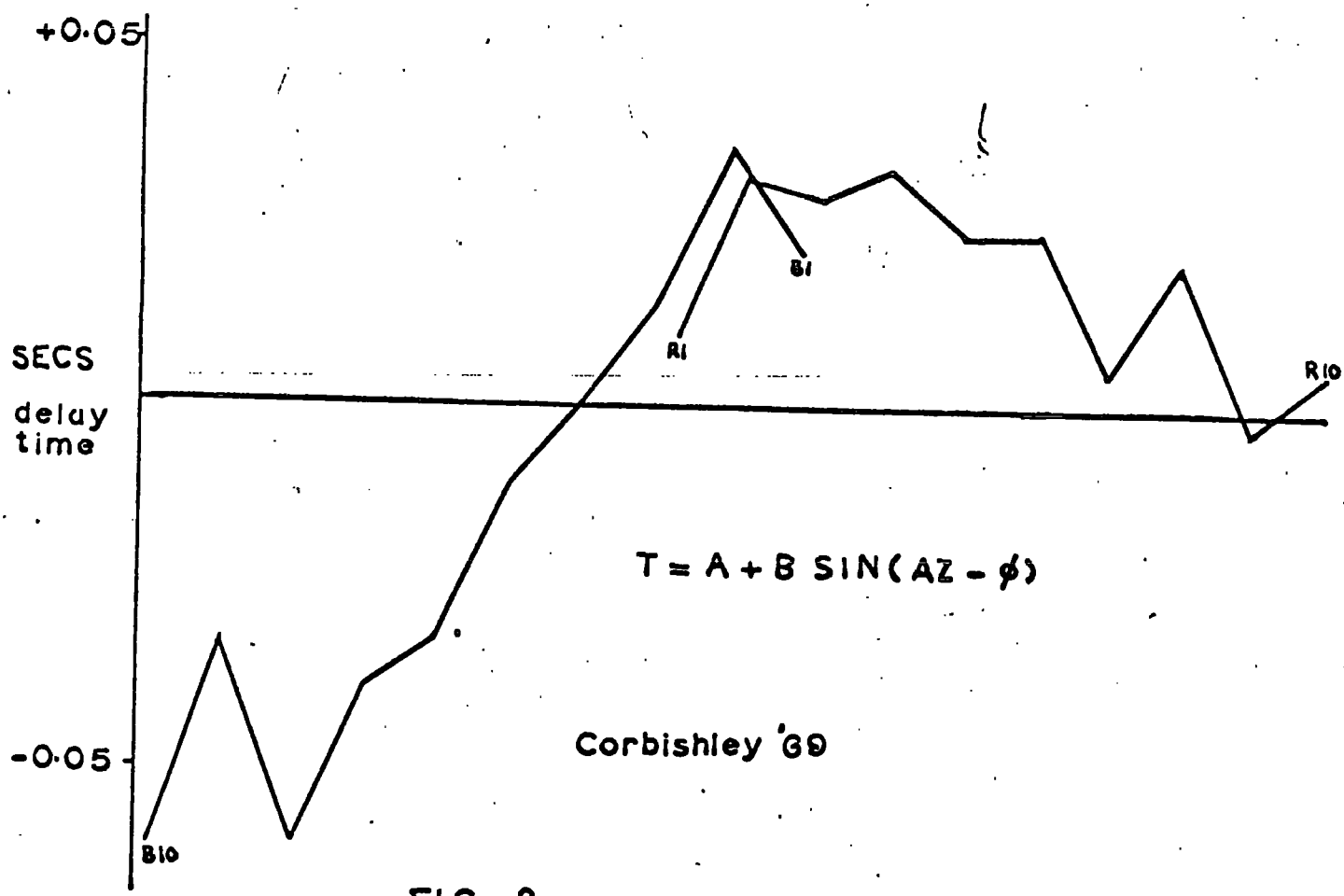
+0·05
SECS
delay
time
-0·05
B10
R1
B1
R10
T = A + B SIN(AZ - ϕ)
Corbishley '69

FIG 2

communication to Greenfield and Sheppard: Bul. Seism. Soc. Amer. 1969 Vol. 59 No. 1] has shown that a series of layers dipping in different directions can give rise to identical residuals to a single layer. So no model deduced from residuals can be unique.

I2 GEOLOGY

The array is situated on a relatively flat alluvial plain. The area where rock outcrops at the surface is a fraction of the total area and consequently the geological evidence is very scanty.

Western and Central Australia were welded into a stable shield area before the end of Precambrian times. Synchronous batholiths and highly metamorphosed sediments in the Kimberley district, West Queensland and to a lesser extent in the Tennant Creek area, is possible evidence of old mountain ranges in these regions. These would have given rise to sediments for three major geosynclines, the Pine Creek, Warramunga and Carpentaria geosynclines. [See Figure 3]

An orogeny at the end of the Lower Proterozoic marked the end of geosynclinal sedimentation and the beginning of the rise of new mountain chains. These mountains were, in turn, eroded in the Upper Proterozoic and sediments were deposited in epi-continental seas. Since then, the region has been covered by shallow seas in Middle Cambrian and Lower Cretacious times but there is no evidence of any further major geological activity.

The Warramunga group is made up of sandstones, siltstone, shales, greywacke and mudstone and is extensively intruded by Precambrian granites. [Reference - The Geology of the Tennant

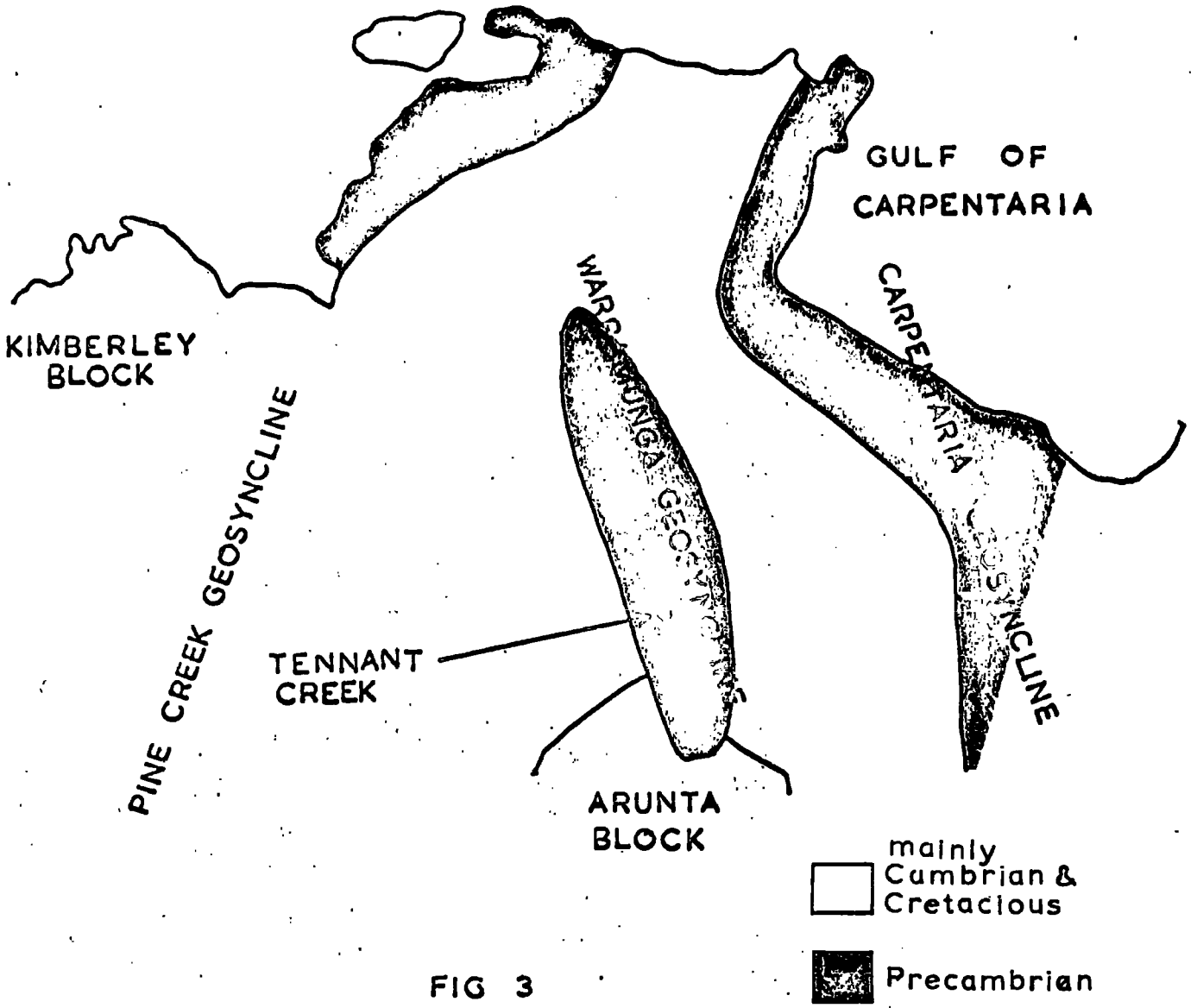
KIMBERLEY BLOCK
PINE CREEK GEOSYNCLINE
TENNANT CREEK
ARUNTA BLOCK
GULF OF CARPENTARIA
mainly Cambrian & Cretacious
Precambrian

FIG 3

Creek One Mile Sheet Area by P. W. Crohn and W. Oldershaw 1965] According to Crohn and Oldershaw, in the region of the array, 3,000 feet of massive sandstone overlies shales and siltstone. The sediments dip outwards from a granite, suggesting that intrusion has thrust aside the surrounding structure.

The existence of a granite complex, south of Tennant Creek and west of the array is known from bore hole data. The major phases are porphyritic adamellite and gneissic granite and the complex encloses several large blocks of Warramunga sediments. The extent of this complex is not known, but in the immediate vicinity of the array, a large granodiorite mass outcrops at the surface.

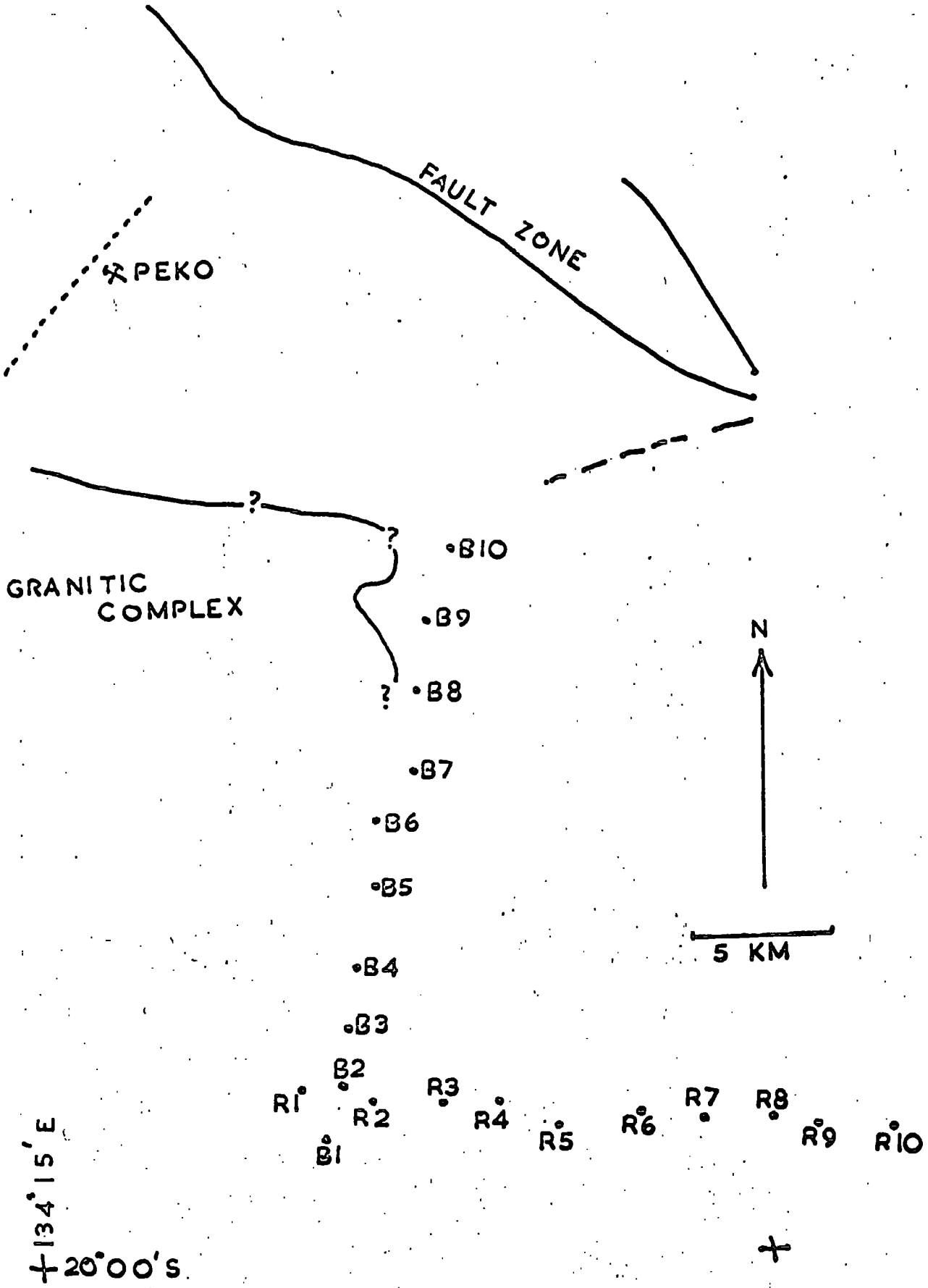
FAULT ZONE
PEKO
GRANITIC COMPLEX
?
?
?
B10
B9
B8
B7
B6
B5
B4
B3
B2
B1
R1
R2
R3
R4
R5
R6
R7
R8
R9
R10
N
5 KM
134°15'E
20°00'S

FIG 4

CHAPTER II

II,1 SURFACE WAVE THEORY RESUMÉ

The displacement vector of an elastic wave in an elastic solid can be expressed as the sum of a vector and scalar field.

$$u = \nabla\phi + \nabla \times \psi$$

The equations of motion of an elastic solid are satisfied if

$$\nabla^2\phi = \frac{1}{\alpha^2} \cdot \frac{\partial^2\phi}{\partial t^2}$$

and

$$\nabla^2\psi = \frac{1}{\beta^2} \cdot \frac{\partial^2\psi}{\partial t^2}$$

α and β are P and S wave velocities in the medium. The general solutions of these equations are

$$\phi_1 = A e^{i(\omega t - kx) - \nu_1 z} + B e^{i(\omega t - kx) + \nu_1 z}$$

$$\psi_1 = C e^{i(\omega t - kx) - \nu_1' z} + D e^{i(\omega t - kx) + \nu_1' z}$$

To obtain an equation of motion for a plane wave propogating in plane layers above an infinite half-space, appropriate boundary conditions are applied to the equations of motion of each individual layer and half-space. The solution is confined to the surface by specifying that amplitude must tend to zero as depth tends to infinity (i.e. B,D = 0 in the half space) and the components of stress in the plane of the surface are zero.

At each interior discontinuity, there are, in general, four boundary conditions [the continuity of two stress and two displacement components]. Each boundary condition gives a homogeneous linear equation in the unknowns, and there are as many equations as there are unknowns. The system of equations has a solution if its determinant vanishes and the determinant

$$\Delta(c,k) = 0 \qquad (X)$$

defines the Rayleigh wave equation.

In the past, the complexities of surface waves have been attributed to imperfections of elasticity, resonance of crustal columns, scattering or a breakdown of classical wave theory. It is now clear (Ewing, Jardensky, Press 1959) that layering is responsible for nearly all surface wave effects. In particular, velocity is a function of period in equation (X), which is the definition of dispersion.

Equation (X) has appeared in the literature in a variety of forms but always as an equation that can be factored and each factor = 0 represents a wave type. Two branches of the function exist corresponding to M_1 and M_2 type propogation. M_1 type particle motion is retrograde elliptical. M_2 type is prograde elliptical.

The Rayleigh wave equation may be expressed in terms of hyperbolic functions. As Tanh x tends to zero, x will tend to an infinite number of π terms. Thus the function remains oscillatory and an infinite number of solutions exist, corresponding to an infinite number of higher modes, subject to the requirement that $\beta_2 > c > \beta_1$. The fundamental Rayleigh mode and the first and second higher modes are usually identified with M_{11}, M_{21}, M_{12} modes respectively. [Mnm where n = 1 or 2, retrograde/prograde; m = mode number.]

At the short and long period limits, the fundamental mode phase velocity tends to the phase velocity in the upper layer and substratum respectively. However, the limiting values for the higher modes are the shear velocity of the upper layer and

substratum.

For the case of a dipping layer or wedge, no exact solution of the Rayleigh wave equation has been developed. It is, therefore, necessary to approximate a dipping structure to one or more constant thickness layers. Various workers have found this approximation to be justified in practice. [Reference: McEvilly and Stavder S. J.; Geophysics Vol. 30, April 1965.]

The amplitude of Rayleigh waves decreases exponentially with depth. A Rayleigh wave of wavelength, λ , is entirely unaffected by the medium at depths greater than λ . Therefore, the dispersed surface wave train gives some indication of the vertical velocity changes in the crust.

A Rayleigh wave train may be considered as resulting from the interference of an infinite number of sinusoidal waves, each travelling with its own particular phase velocity. The dispersed wave packet will be continuously changing with time and a peak with a certain period and group velocity will continually reappear as its component sinusoids go through a cycle of constructive and destructive interference.

The equation for phase velocity [Reference - Brune, Nafe and Oliver - Journal Geophys. Res. Vol. 65. pp.288] is

$$Ct - x = \left(N \pm \frac{1}{8} - \frac{\phi_o}{2\pi}\right)\lambda$$

[ϕ_o is the source phase, N is an integer corresponding to the number of interference cycles over the propogation time t]

Unless phase at the source is known or neglected, phase velocity can only be obtained by an inter-station method.

$$c = \frac{\Delta x}{\Delta t - NT} \qquad (Y)$$

Δx = distance between two seismometers.

Δt = difference in arrival time.

T = period, N = integer.

II,2 PHASE AND GROUP VELOCITY: PRELIMINARY DETERMINATIONS

Figure 5 shows an arrival at the array of a blast at Peko mine which is thirty kilometres north of the array cross-over point, and Figure 6 the same signal after filtering. P, S and Rayleigh wave arrivals are clearly visible, and the dispersive nature of the surface waves is apparent from Figure 6. No Love wave mode can be present on the record, as the array consists entirely of vertical instruments and there is no vertical component of particle motion in Love wave propogation.

Fifteen Peko events were selected from the 1967 hellicorder records. The analogue information was played out from twenty-four track magnetic tape. The band-pass filters available had a 24 decibell per octave roll off and the records were filtered at a half to four cycles per second. Graph 7 shows the phase response of the filters.

The location of the events was checked by calculating arrival times of S and P waves assuming Underwood's model and an origin at Peko and comparing observed and calculated arrival times. Agreement to within one kilometre was obtained in all cases and this was considered sufficient confirmation of a Peko origin, particularly as no other mines nearby were believed to be operational.

Underwood obtained agreement between observed and calculated arrival times to within 0.01 seconds using equation (Z) and his postulated model values.

$$T.T. = (2h \cos\theta + \Delta_j \cos\phi_j \sin\theta)\frac{\cos i}{V_1} \quad \text{(travel time)}$$

$$+ \frac{\Delta_j}{V_2}(1-\cos^2\phi \sin^2\theta)^{1/2}$$

$$\phi_j = \underset{\substack{\text{DIP DN}\\ 205.5^\circ}}{\Phi_o} - \underset{\substack{\text{baring of}\\ j^{th}\text{ pit}}}{\Phi_j} \qquad (Z)$$

PIT NÖ

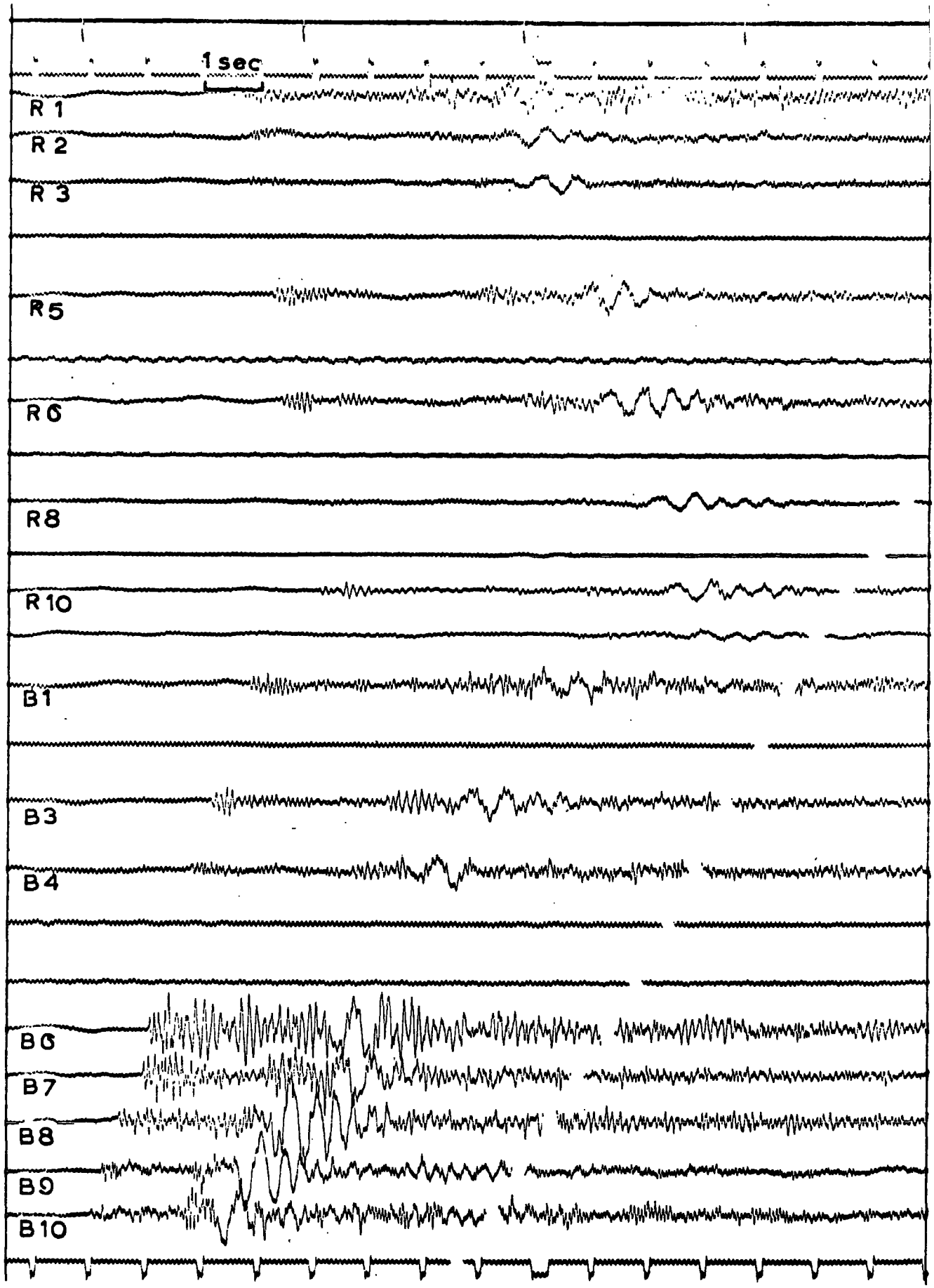

FIG 5

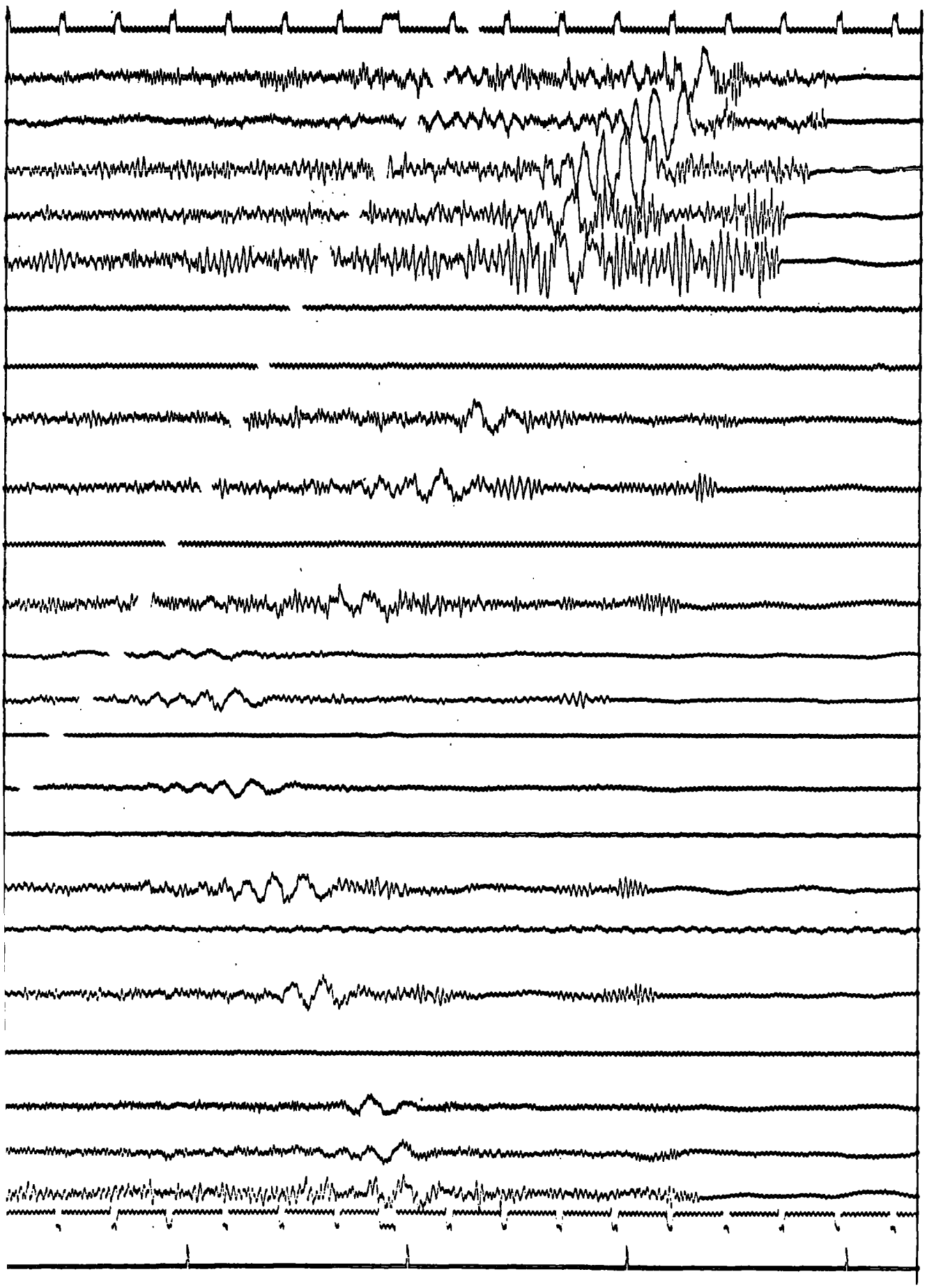

PIT NÖ

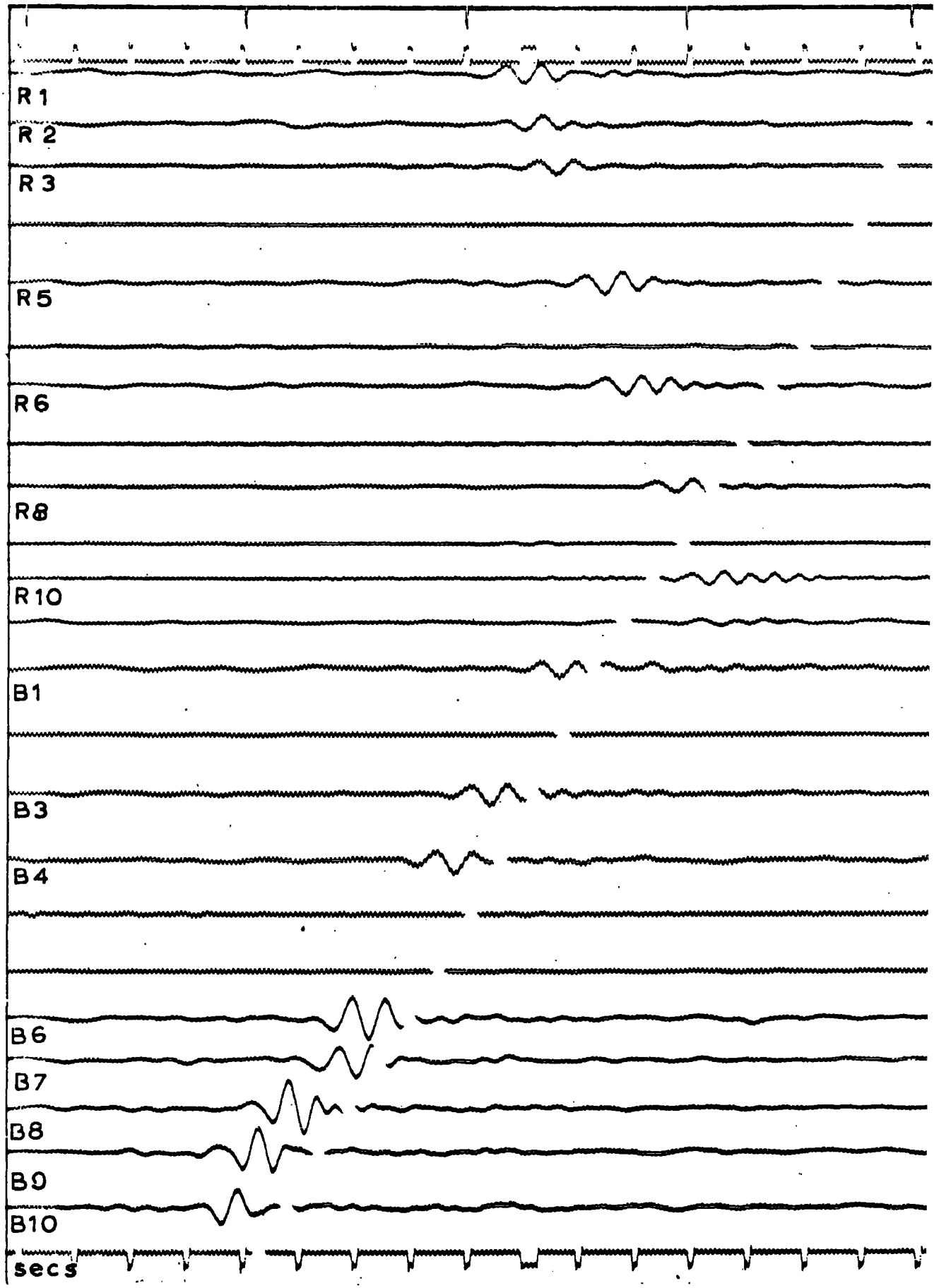

FIG 6

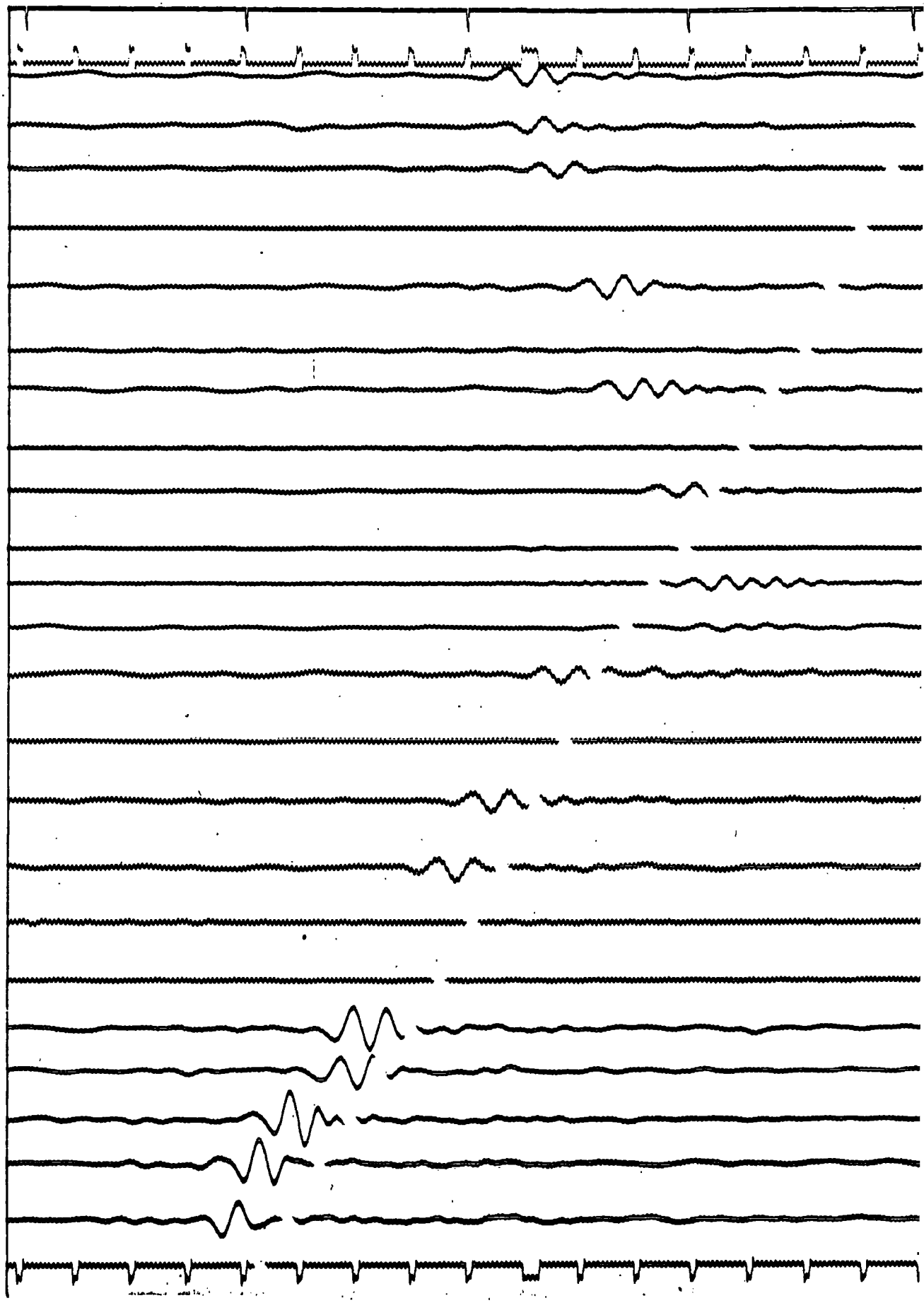

FIG 7

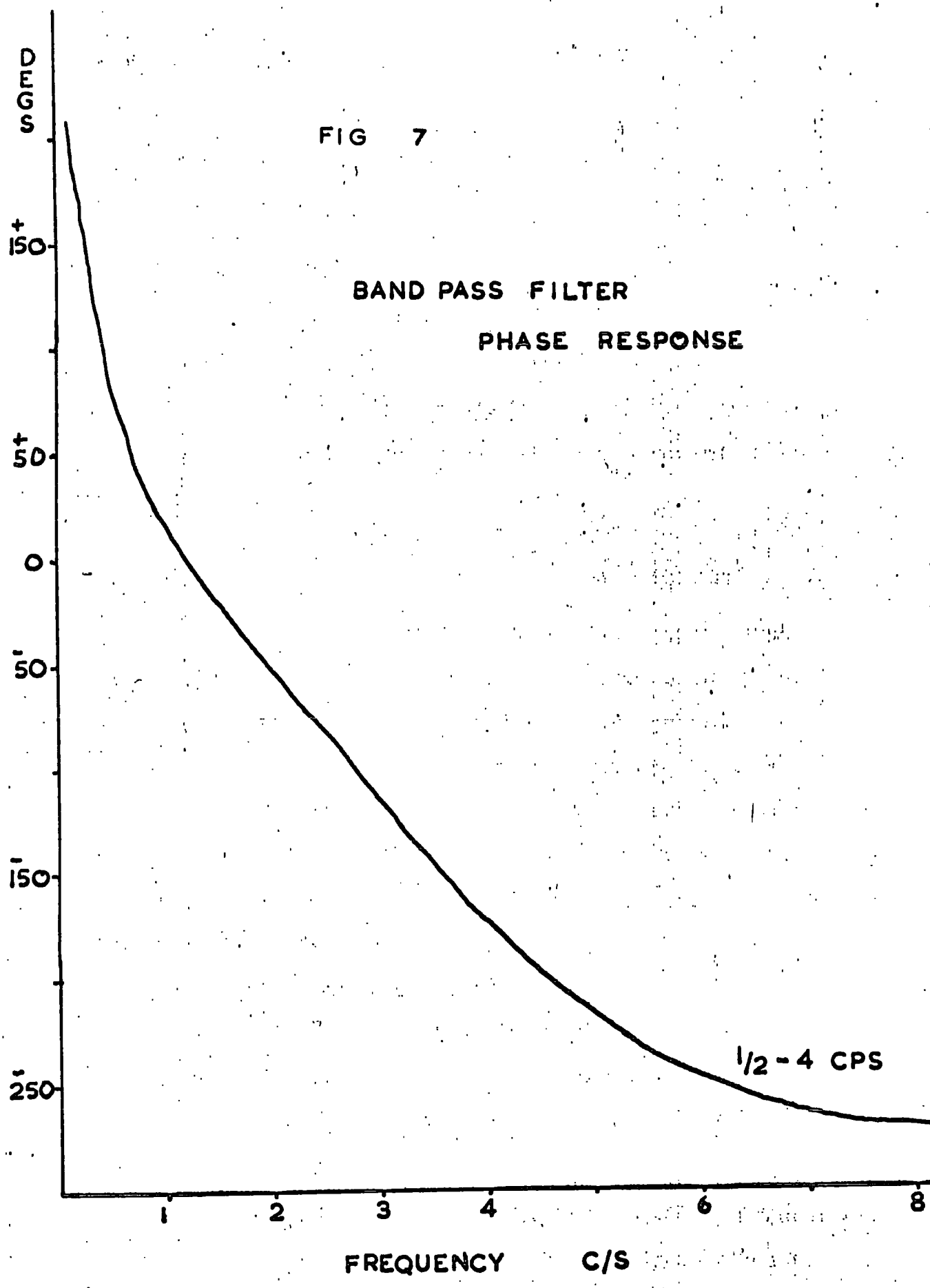

BAND PASS FILTER

PHASE RESPONSE

h = depth under shot

Δ_j = distance to j^{th} pit

θ = true dip

V_1 = 5.42 kilometres per second

V_2 = 6.10 kilometres per second

Using equation (Z) for the Peko events, the calculated and observed difference in arrival times at separate pits agreed to within $\pm$ 0.15 seconds. Therefore the origin time of the events, calculated from (Z) was assumed to be 2.75 seconds prior to the arrival of the P wave at B10 with an error of $\pm$ 0.10 seconds.

GROUP VELOCITY

Normally, the most accurate method of measuring arrival times and periods from a seismogram is to number the peaks in the dispersion wave pocket, plot peak number against arrival time of the peaks, and smooth. The gradient of the tangent to a point on the smoothed curve is the period corresponding to a particular arrival time. This method was not found to be satisfactory for this very short period data. Any deviations from a smoothed curve are, in theory, due to measuring inaccuracies or minor heterogeneities in the earth's crust. For very near surface dispersion, it is less likely that crustal heterogeneities will be minor, and smoothing at this stage lead to large errors in the period values, particularly as the periods varied very little. If higher modes were present, a less regular wave train would be expected, and smoothing might have distorted the data. In addition, there was considerable uncertainty in the numbering

of the peaks in regions of low signal to noise ratio.

In preference, a method suggested by Crampin [Higher Modes of Seismic Surface Waves Geophys. Journal Vol. 9, 1964] was used. This is not only more exact but provides a direct measure of the errors inherent in the analysis. The period and arrival time of each crest was measured separately and plotted. Figure 8 shows the plot for nine events at pit Blue One. This graph was then smoothed and the values from the smoothed curve used to plot a group velocity against period graph. Figure 8 gives a direct impression of the errors in the interpretation and defines the error bars in Figure 9.

DISCUSSION OF ERRORS

A certain scatter in the arrival time vs period graph is inherent in the method because arrival time is not necessarily equidistant between two crests. This error was estimated as $\pm$ 0.1 seconds. The seismograms were measured to an accuracy of $\pm$ 0.05 seconds. This is a figure embracing the noisiest portions of the trace. $\pm$ 0.02 is a more average estimate.

The error in origin time of $\pm$ 0.1 seconds has already been mentioned. The phase at the source can lead to significant crest displacements, particularly for deep events. Although the origin time is related to the epi-centre, a Rayleigh wave is not considered to exist until the compressional wave reaches the surface, or until $x > h \tan \theta$ [see diagram and Ewing, Jardensky, Press p.60]

GROUP VELOCITY PLOT
CRAMPIN'S METHOD

PIT BLUE 1

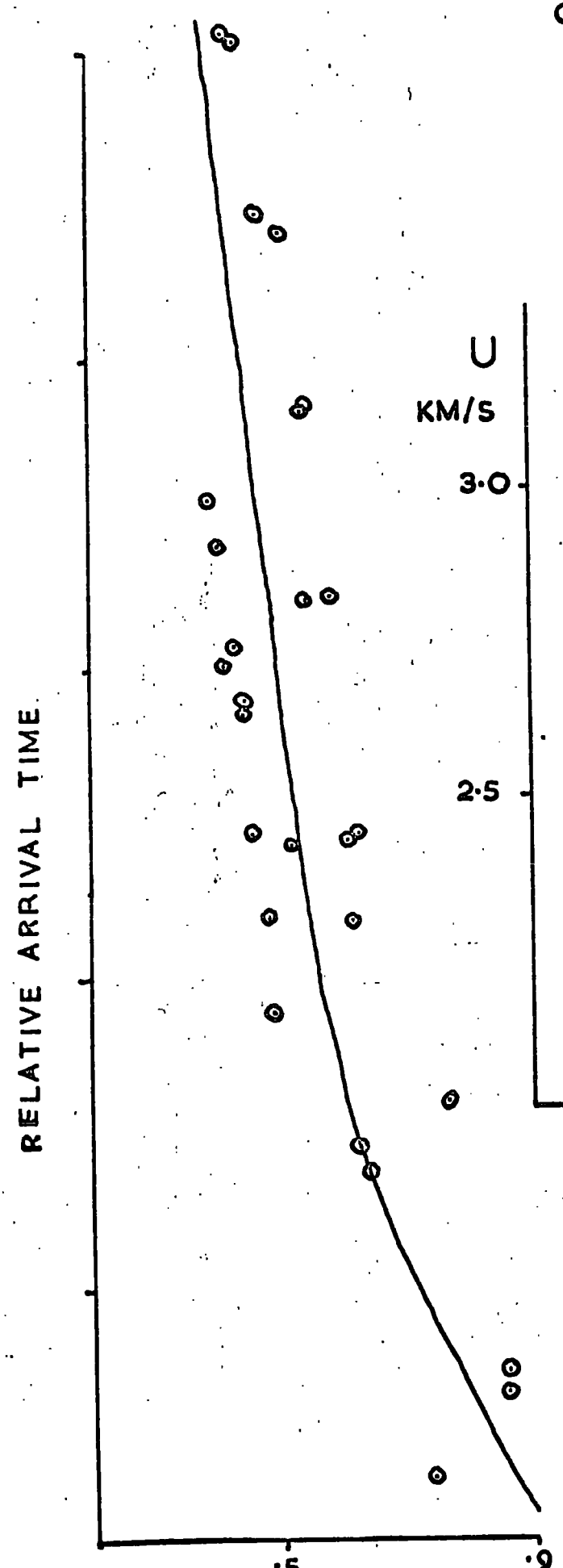

FIG 8

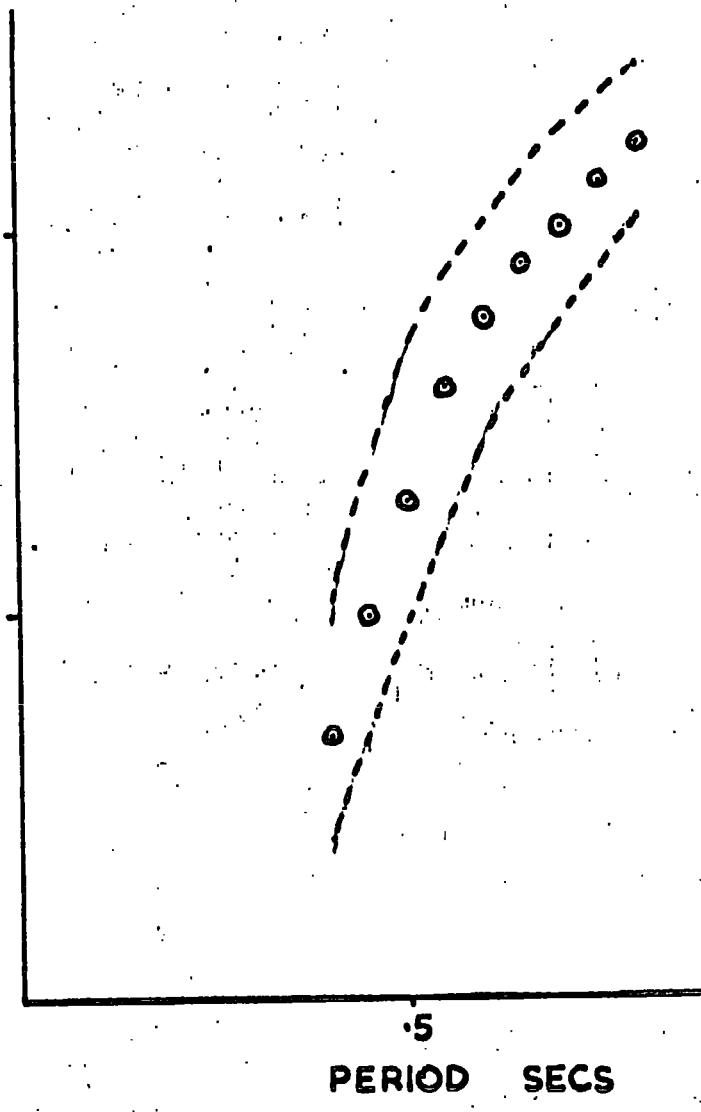

FIG 9

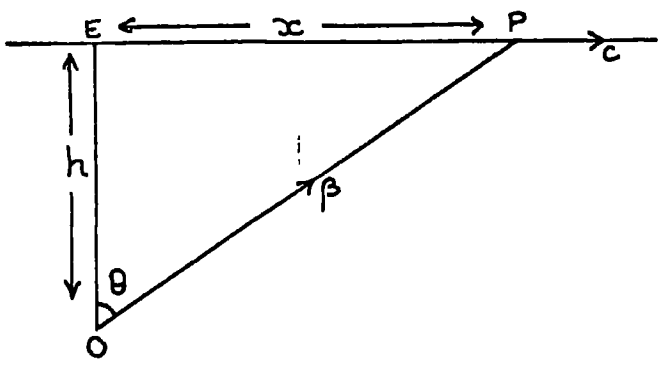

The source phase is related to position P. This error is known to be small and in this experiment was neglected. [h assumed to be small.]

The phase shifts due to variations in the seismometer characteristics would introduce further error. Muirhead (PhD thesis 1967) carried out a computer simulation of the Willmore Mk II phase response and found that an error of 0.04 seconds may be introduced for a signal of frequency 1 cps. The phase response of the filters used in the playout equipment are shown in Figure 7. The data has been corrected for this shift. Previous workers have checked the equipment for pen misalignment and the possible snaking of the tape past the pick-up heads, and have found the errors to be insignificant.

Any heterogeneity in the crust, causing reflections and refractions, or any anisotropy, will give rise to further scatter. This is to be expected for the near surface structure under investigation. There may also have been slight differences in location of the events throughout Peko mine and therefor slightly different propogation paths.

Near to an event, the surface wave packet is effectively a fourier transform of the source function. As the wave progresses, the different modes separate out. The array is too close to

Peko for any mode separation to be immediately apparent. The wave packet may represent the summation of the sinusoids from various modes. Therefore it is reasonable to expect a scatter in period from a smoothed curve.

INTERPRETATION

Figures 10-13 show the group velocity curves for all the seismometers. The only trend that emerges [see Figure 8-9] is a possible lower near surface (short period) velocity to the north of B6 than to the south. The fall in the upper limit cut off at B8 and B9 simply reflects the fact that short periods emerge first from the transform of the source function and B9 is a mere 17 kilometres from the mine.

As already mentioned in Chapter One, a granite complex enclosing large blocks of Warramunga Sediments exists to the west of the array. Maps prepared by the Bureau of Mineral Resourses, Australia, tentatively draw in the eastern boundary of this complex in the region of the array. It is possible that the lower near surface velocities of B6, B7, B8 and B9 may be attributable to a granite free propogation path.

A programme developed by Harkrider was used to obtain theoretical dispersion curves for Rayleigh waves propogating through a defined horizontal layered crustal model. [See Appendix A.] The density used in the computer models was 2.8 g/cc, constant over the depths considered. Figure 14 shows a number of theoretical curves superimposed on the Blue One group velocity confidence limits. A component wave with a period T and velocity C will have a wavelength of (C x T). Due to the exponential decay of amplitude with depth, it is generally

GROUP VEL DISPERSION CURVES

Crampin's Method

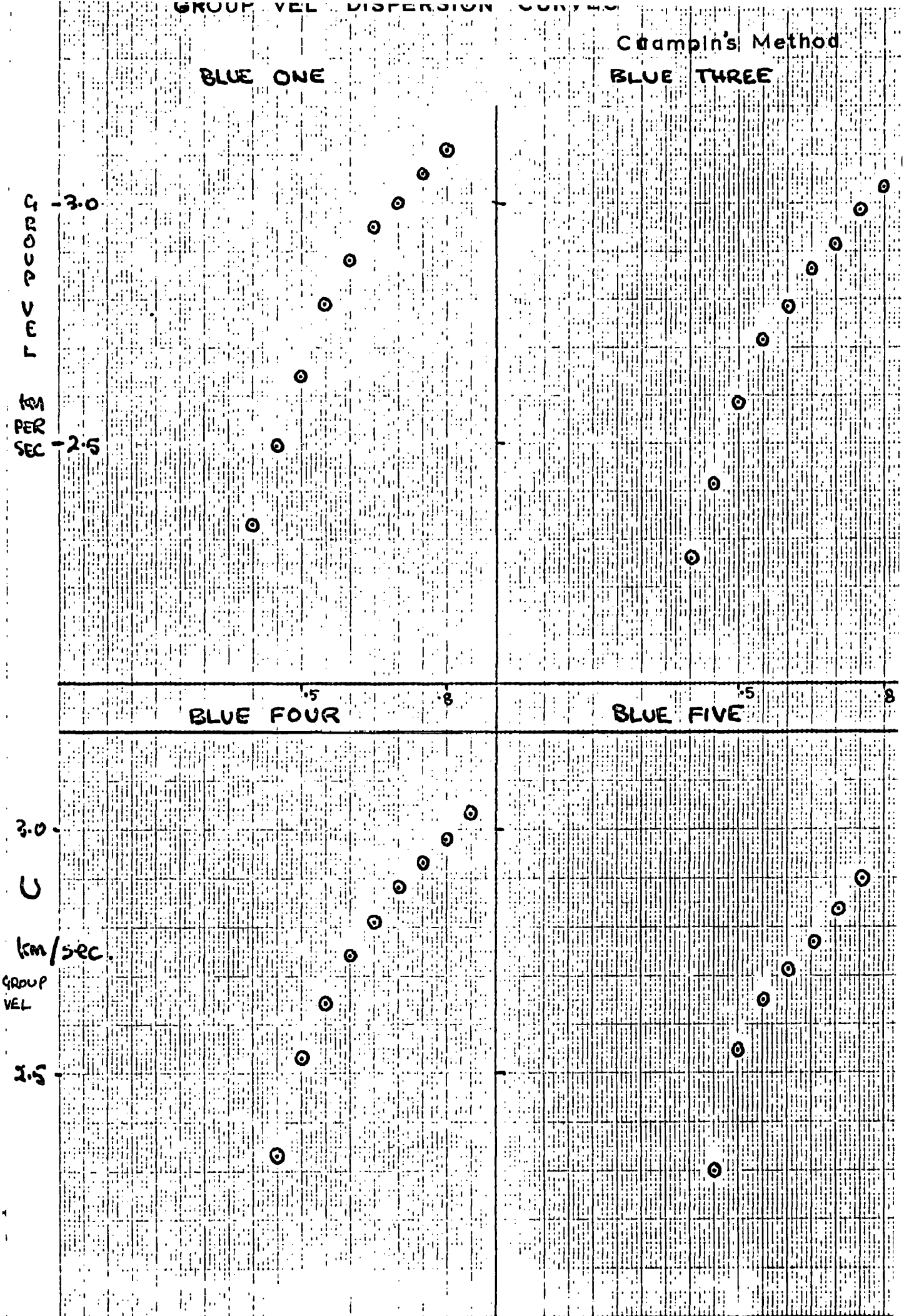

FIG 10

FIG 11

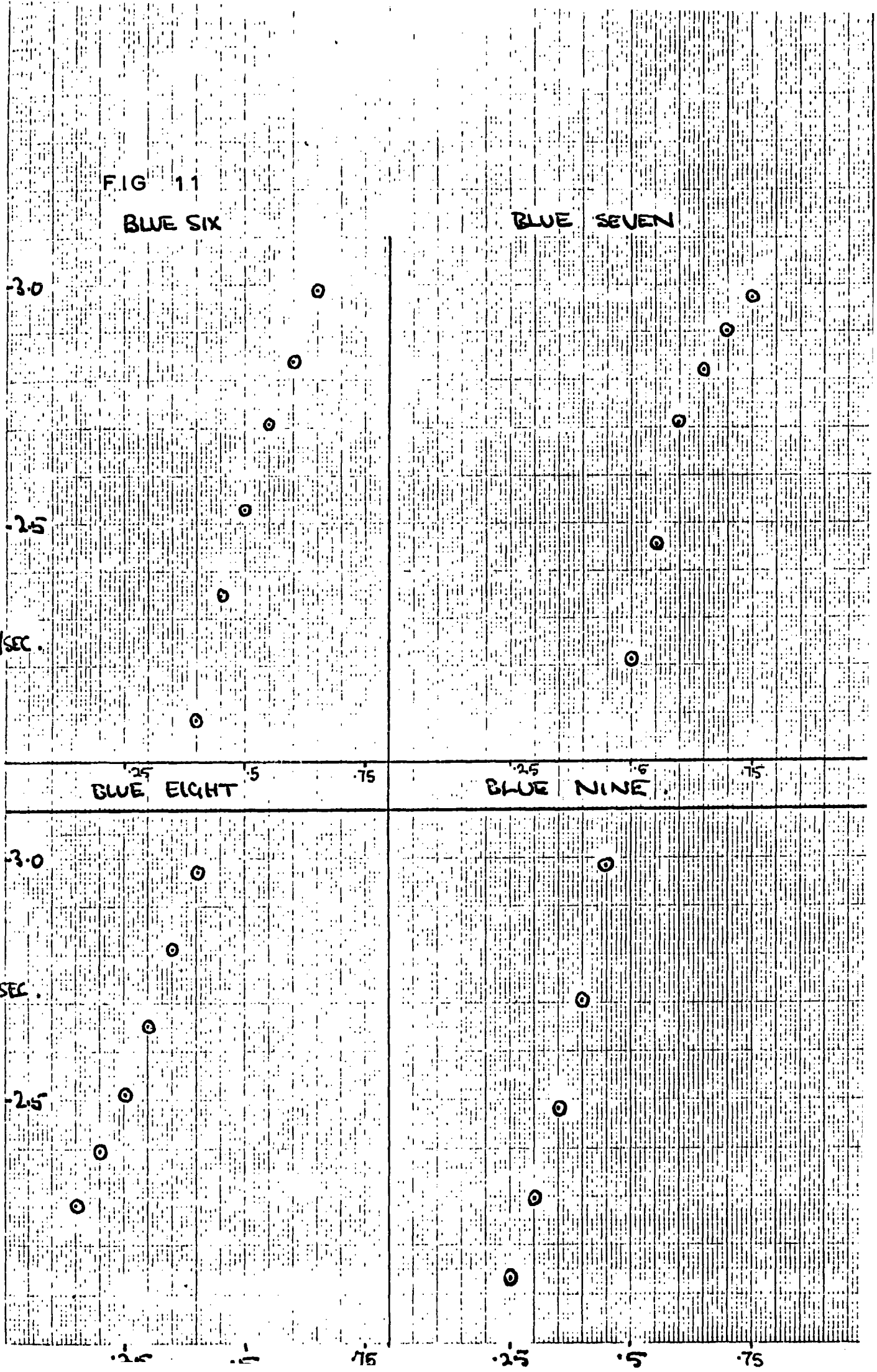
BLUE SIX
BLUE SEVEN
BLUE EIGHT
BLUE NINE
3.0
2.5
GROUP VEL
KM/SEC.
U
.25
.5
.75
.6

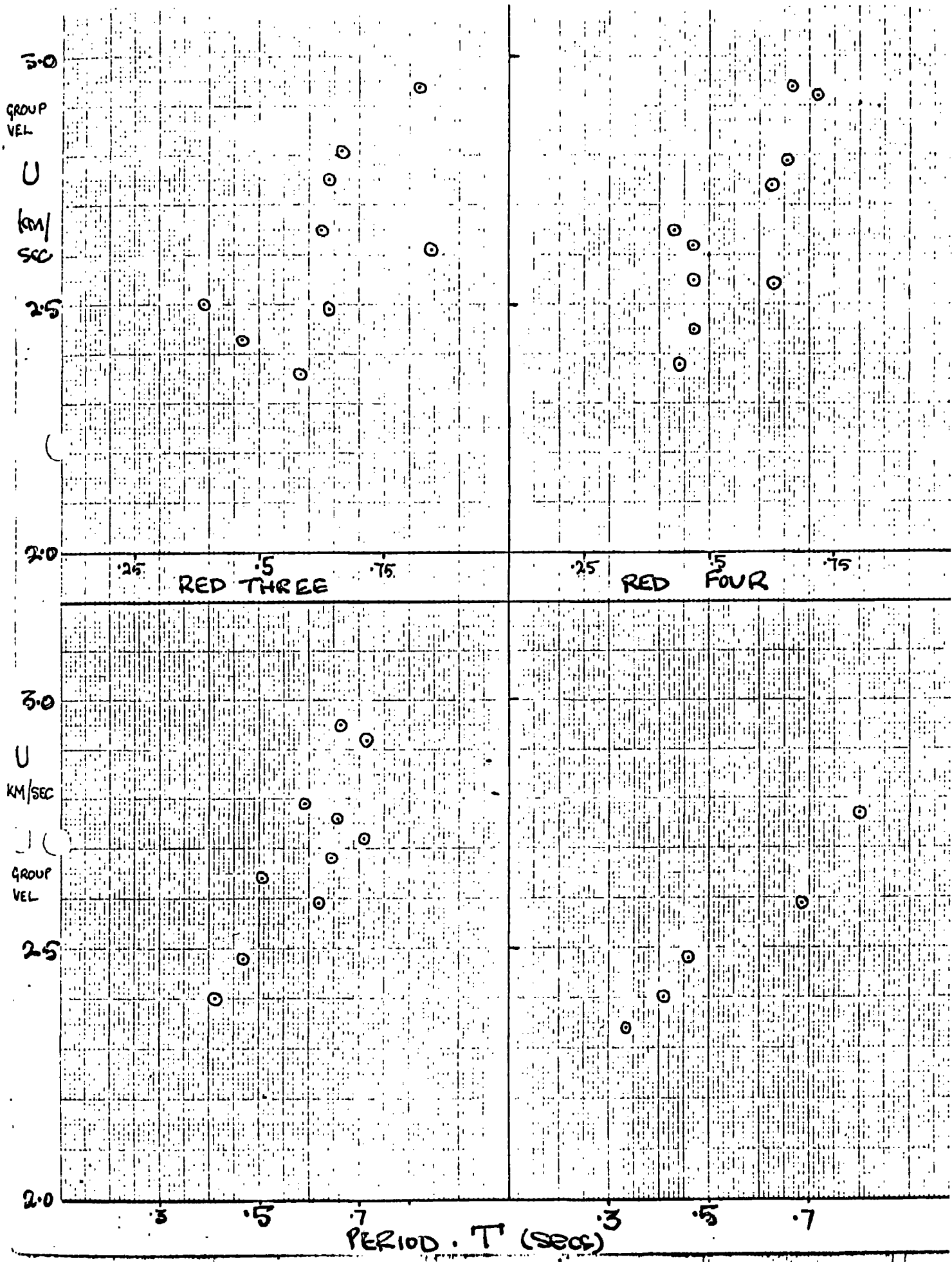
3·0
GROUP VEL
U
KM/SEC
2·5
2·0
·25
·5
·75
RED THREE
RED FOUR
3·0
U
KM/SEC
GROUP VEL
2·5
2·0
·3
·5
·7
PERIOD . T (SECS)

FIG 12

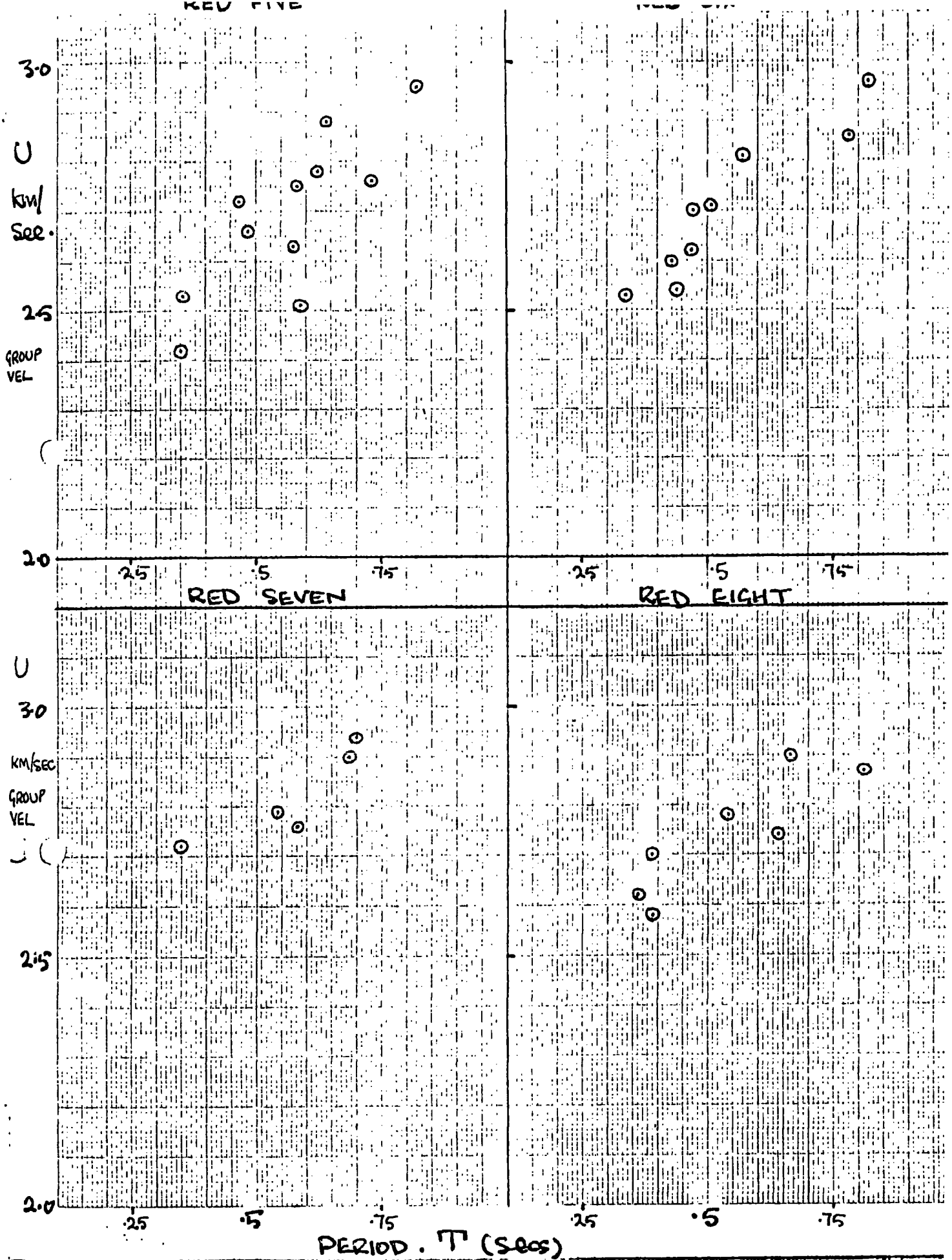
RED FIVE
RED EIGHT
RED SEVEN
U
KM/SEC
GROUP VEL
3.0
2.5
2.0
.25
.5
.75
PERIOD . T (SECS)

FIG 13

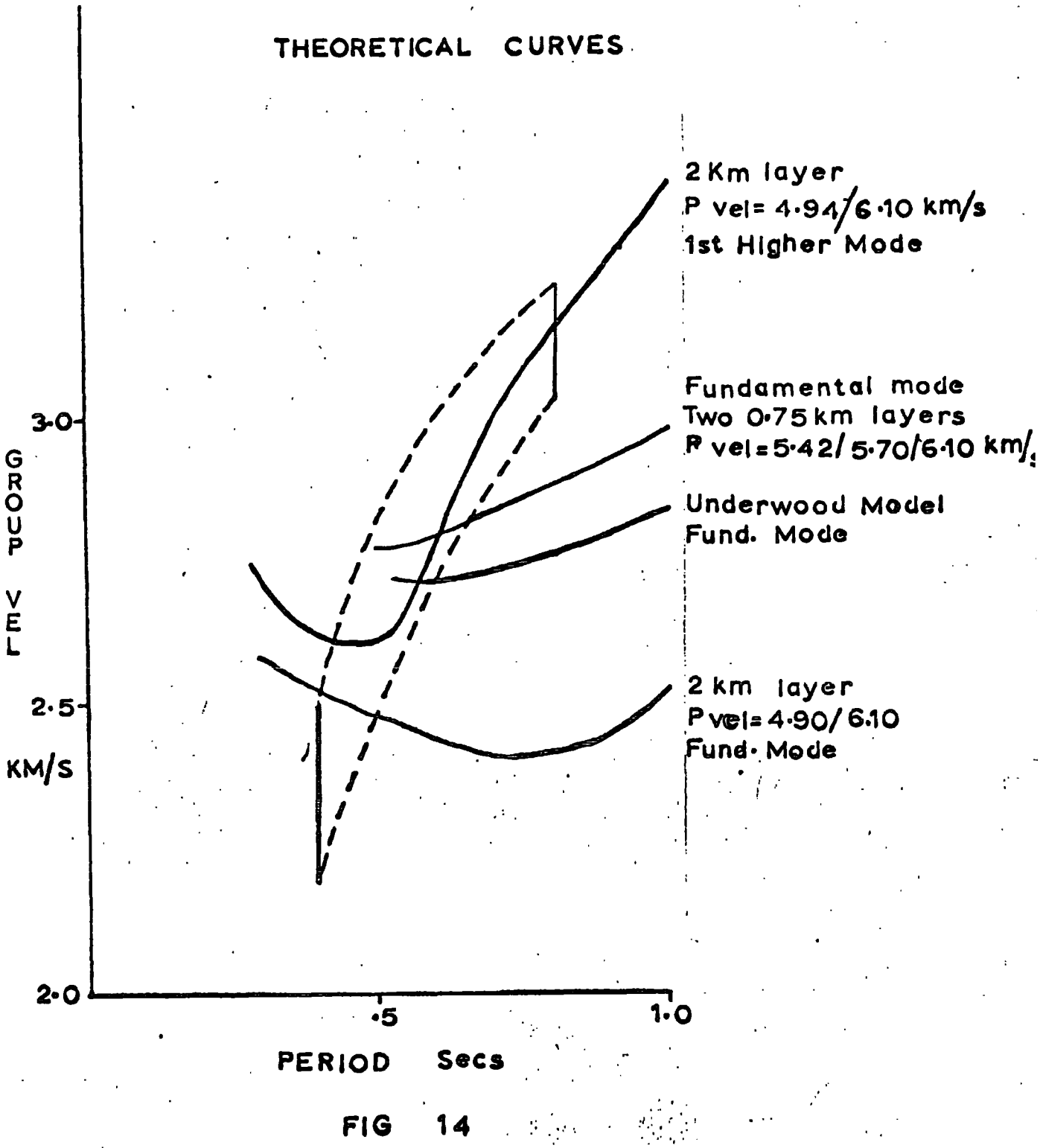
THEORETICAL CURVES
2 Km layer
P vel= 4·94/6·10 km/s
1st Higher Mode
Fundamental mode
Two 0·75 km layers
P vel=5·42/5·70/6·10 km/s
Underwood Model
Fund. Mode
2 km layer
P vel= 4·90/6.10
Fund· Mode
GROUP VEL
KM/S
3·0
2·5
2·0
·5
1·0
PERIOD Secs

FIG 14

assumed that the wave propogates through a surface layer which is approximately ($^2/_3$ x C x T) kilometres thick. Therefore, the depth of interest in this problem was roughly three kilometres.

All the fundamental mode models tried, tended to have their characteristic group velocity minima in the period range considered. It is a common feature of seismograms that the envelope of waves with the maximum energy is associated with a minimum of group velocity. This is simply because, in the region of a turning point, a wide band of periods have approximately the same velocity and hence the same arrival time. This maximum amplitude peak (or peaks) is known as the Airy phase.

It is therefore encouraging that the crests with maximum amplitude for this data correspond to the group velocity minimum of a dispersion curve for an expected average crustal model. This is not to say that all the computed points can simply be considered as Airy phase. Near to the source, the source function transform and the Airy Phase are as one. As the wave progresses, the different frequencies are effectively emerging from the Airy Phase.

Figure 14 shows that the best but by no means unique fit to the data were with a first higher mode. In fact no fundamental mode model gave rise to the required curve steepness over the period range considered. This suggests that the dominant mode emerging from the Airy phase may be the first Rayleigh mode.

So the smoothed curves of Figures 10-13 should not be considered as the dispersion curves of one mode. Rather, they are more likely to be an average plot of the identifiable arrivals; the Airy phase, possibly the first higher mode, and in theory

an infinite number of higher modes that may or may not be detectable. The prominence of different modes may also vary from one event to another.

The experiment would have been greatly enhanced if some method of positive mode identification had been possible. The simplest method would have been to observe the relative particle motions in the propogated wave with a three component set of seismometers. However, no three component set was available.

PHASE VELOCITY

By virtue of the method of calculation, [see equation Y] inter-station phase velocity is a function of the structure between the two stations. Considering the earth as a filter:

$$f_2(t) = H(p)\ f_1(t)$$

where $H(p)$ is the crustal transfer function.

$f_2(t)$ = signal at output : seismometer 2.

$f_1(t)$ = signal at input : seismometer 1.

The event should be in line with the seismometers. However, in this experiment, ray paths to two adjacent seismometers only diverged by approximately 3 degrees. So it was assumed that the crustal transfer function was constant over this limited arc.

Twelve events were used to obtain phase velocity dispersion plots corresponding to : B1 to B3, B3 to B4, B4 to B5, B5 to B6, B6 to B7, B7 to B8, B8 to B9, B9 to B10. A large scatter was obtained on all the graphs, effectively masking any possible dispersion trend and rendering the graphs uninterpretable. The available frequency bandwidth was rarely greater than 0.4 to 0.9 seconds. This strictly limits any analysis because only a small

portion of a dispersion curve may be identified. As the distance from the source increases, more frequencies separate out and the increased bandwidth leads to a more complete dispersion curve.

Apart from the phase at the source error which cancels out, causes of scatter would be the same as for group velocity. It was assumed that the distance between pits was not sufficient for the next interference cycle to have emerged and so N in equation (Y) was always put equal to zero.

Most of the wide scatter may be attributed to the measurement error. Since a difference of two values was being measured, the limits quoted of $\pm$ 0.02 and $\pm$ 0.05 seconds become, by the summation of errors $\pm$ 0.03 and $\pm$ 0.07 seconds and this gives rise to possible velocity uncertainties of 0.06 and 0.15 kilometres per second respectively.

In this chapter, the limitations of standard eye-ball techniques applied to near event, short period data have been discussed. So far, all that has been revealed is a suggestion that the surface wave dispersion might have resulted from a structure approximating to the Underwood model. For the remainder of the study, the techniques of fourier analysis and velocity filtering were applied to the data in an attempt to increase the observable bandwidth and separate out the modes.

CHAPTER III

III,1 THE SEPARATION OF MODES BY VELOCITY FILTERING

The fundamental requirement for any further analysis is the separation of the modes. Essentially, the modes differ in velocity, and an array of seismometers enables data to be filtered in azimuth and velocity using delay/sum/correlation techniques. No sharp correlation would be expected, since the surface wave velocities varied over the array area. However, summation results in a signal to noise gain of $\sqrt{N}$, where N is the number of seismometers [gain approximately 4.3 for Warramunga] and it was hoped that arrivals disguised in the noise might be revealed.

Velocity filtering was carried out, using a specialised hybrid computer, the Aldermaston Seismic Array Data Analyser (SADA). See Appendix B1. Runs were carried out for two events, with and without initial filtering at a half to four cycles per second. Figures 15 and 16 show two of the outputs. Figure 15 shows correlation centred at 3.1 kilometres per second and slight correlation around 2.2 to 2.4 kilometres per second. The same trend is reflected in the unfiltered total sums of Figure 16.

It is tempting to interpret these results as evidence of two modes. However, SADA assumes a plane wave front whereas the azimuths from Peko to different pits vary by up to 37 degrees. So, a curved wave front modification was written into the SADA programme [see Appendix B2] and the two events were run again. The dominant wave packet still correlated strongly at approximately 3.1 kilometres per second. The second correlation was less well defined but still observable.

FIG 15

SADA FILTERED PRODUCTS

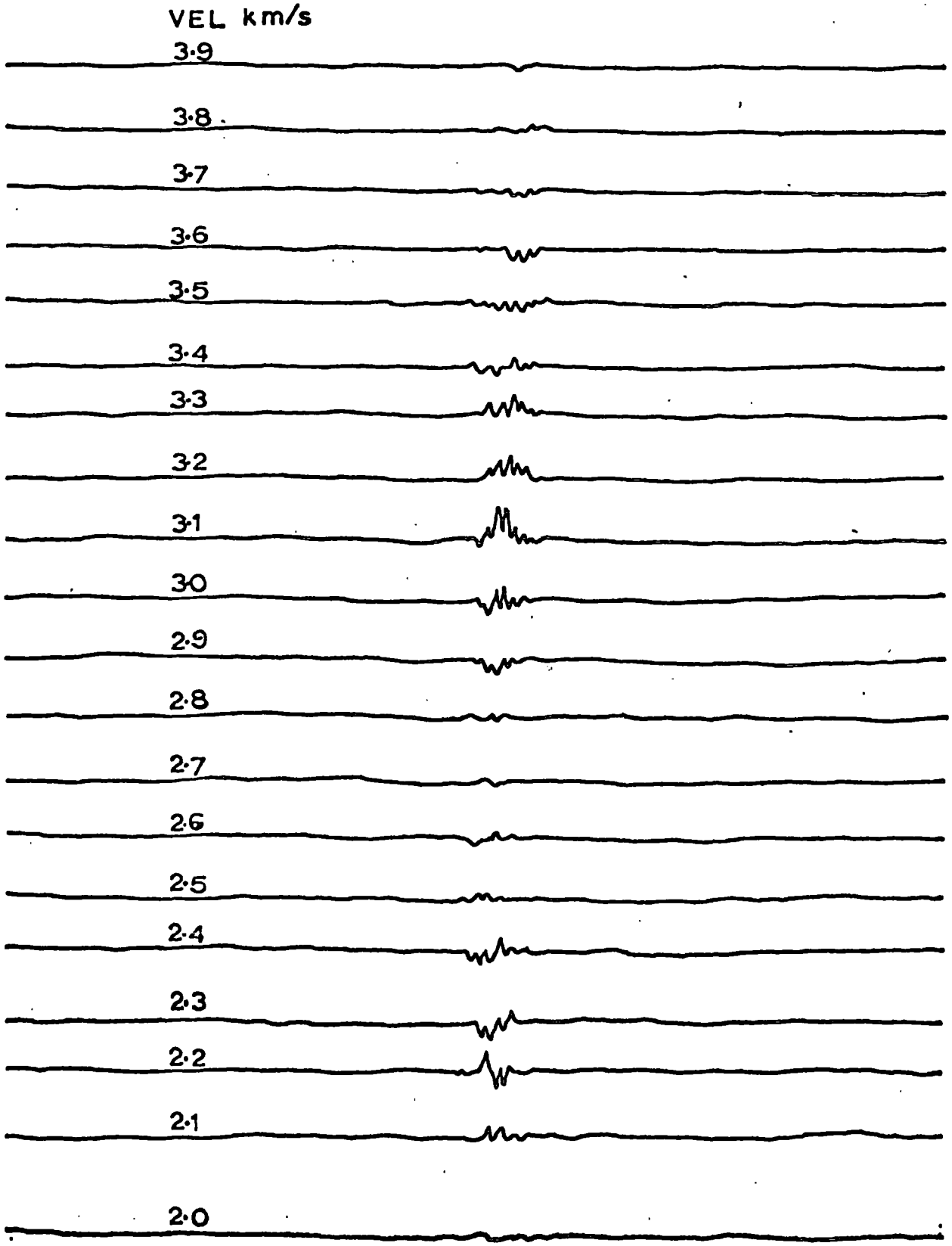

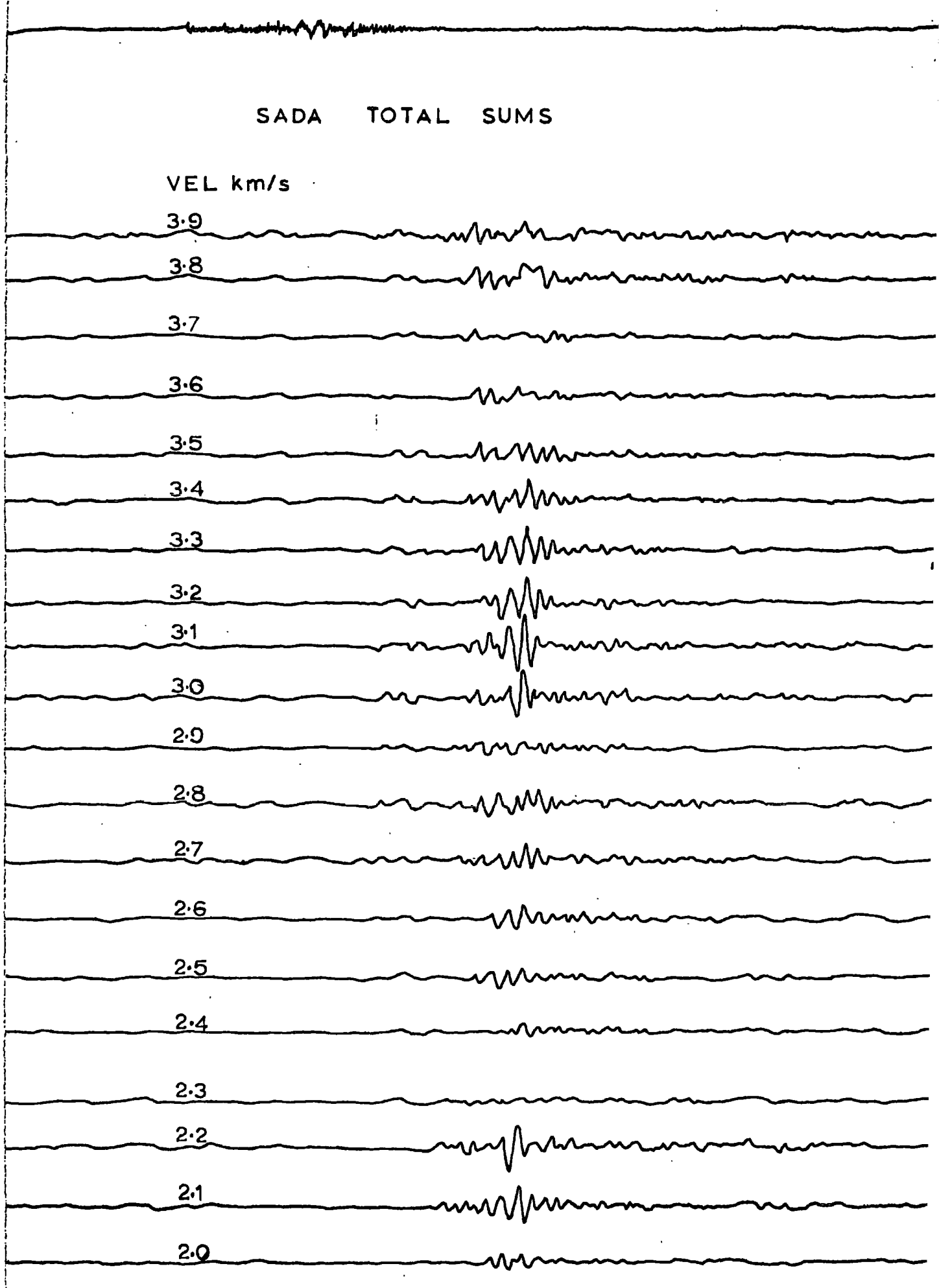
SADA TOTAL SUMS
VEL km/s
3·9
3·8
3·7
3·6
3·5
3·4
3·3
3·2
3·1
3·0
2·9
2·8
2·7
2·6
2·5
2·4
2·3
2·2
2·1
2·0

FIG 16

It is possible that the secondary peak could be due to coherent noise or a refraction of the surface wave at some major vertical structural discontinuity. However, subject to this uncertainty, it is tentatively concluded that the lower velocity peak may correspond to the fundamental mode and the major correlation to the dominant first Rayleigh mode. The actual velocity values have little significance as they only represent some kind of weighted mean over the entire area of interest.

III,2 GROUP VELOCITY DETERMINATION BY FOURIER METHODS

A technique capable of resolving complex signals which are composed of several periods, arriving at a recording station almost simultaneously has been developed by Dzienonski, Bloch and Landismann [Bull. Seism. Soc. Am. Feb. 1969]. In addition, the fourier analysis incorporated in the method enables broader portions of the dispersion present to be recovered than is observable by eye. Two Peko events were analysed using a programme based on this method which was written by C. Blamey and A. Douglas [UKAEA Blacknest].

The seismograms, filtered at a half to four cycles per second were digitised at an interval at 0.078 seconds. It would have been preferable to avoid the phase distortion caused by filtering, for at the time of use, no instrument correction option had been written into the programme. However, the nuiquist frequency sampling interval required for an unfiltered record would have been outside the limits of the equipment available. The traces at each pit in the array were analysed separately.

AMPLITUDE SPECTRA

Figure 17 shows the amplitude spectra of an event for signals arriving at pits B1, B3, B4, B6, B8, B9, R1, R5 and R9. The instability at high frequencies is due to digitising error. The Rayleigh wave energy is peaked at approximately 1.5 cycles per second and the sharp decrease in amplitude to the right of the peak is due to the high frequency cut off of the play out filter. All spectra have a minimum at approximately 0.7 cycles per second and a secondary peak at the lowerfrequency end of the

AMPLITUDE SPECTRA

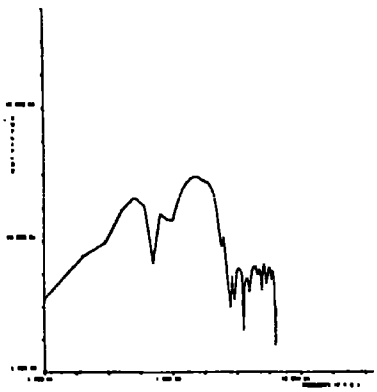

B 6

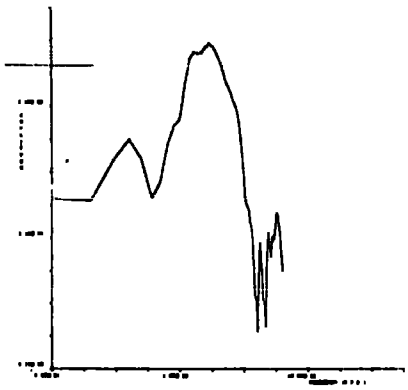

B 8

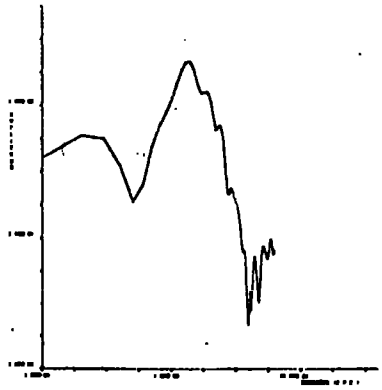

B 9

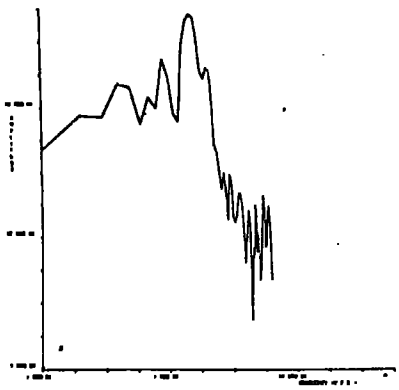

B 1

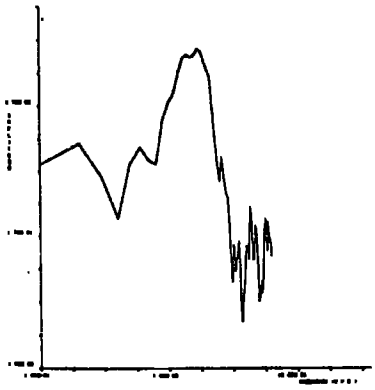

B 3

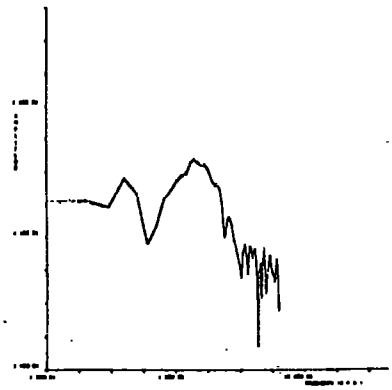

B 4

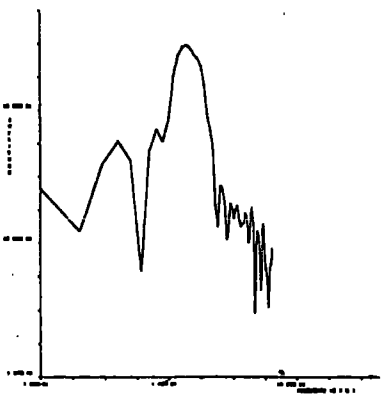

R 1

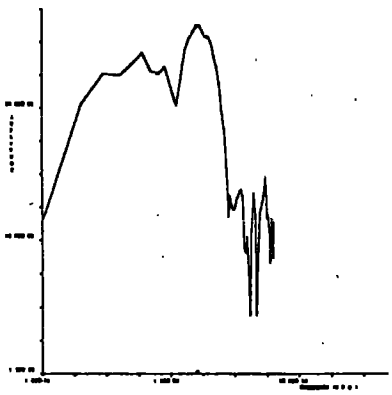

R 5

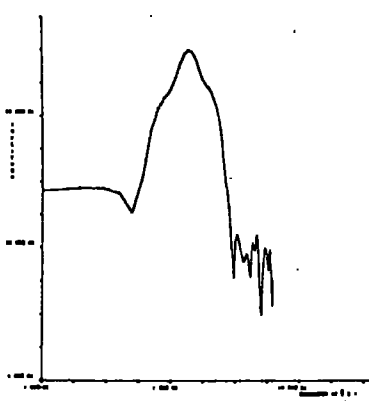

R 9

FIG 17

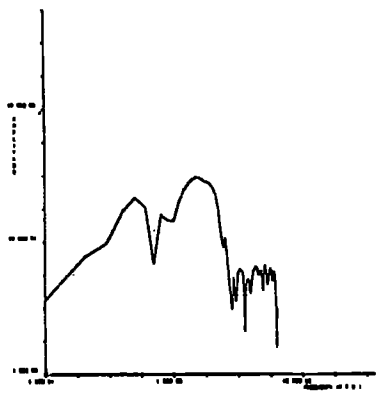

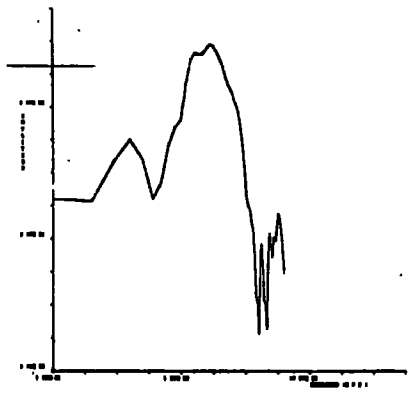

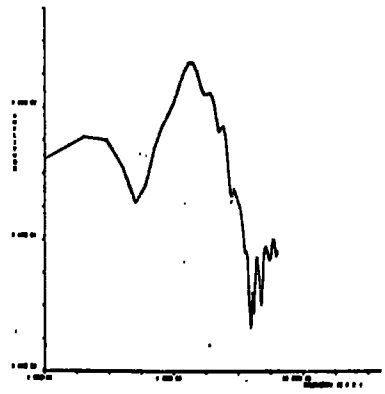

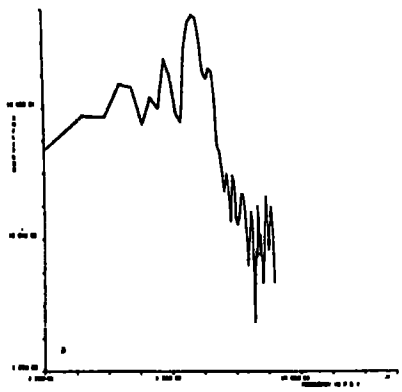

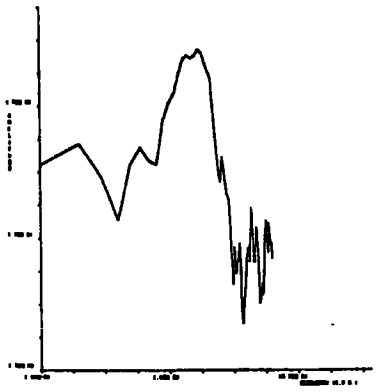

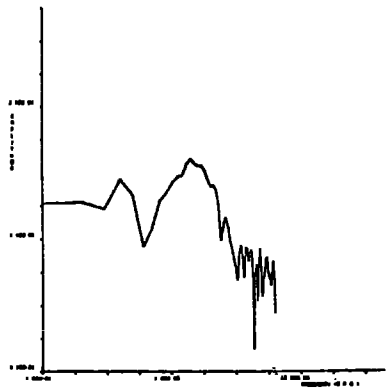

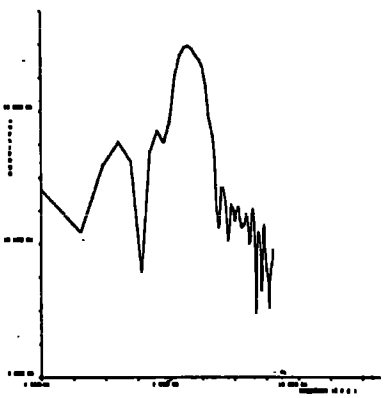

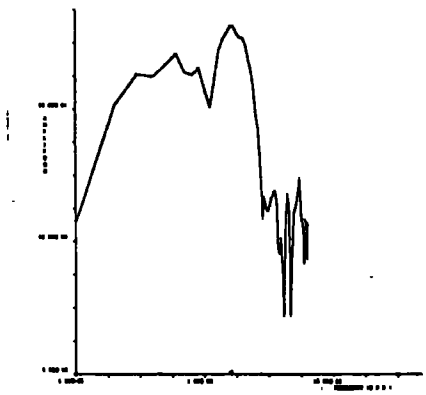

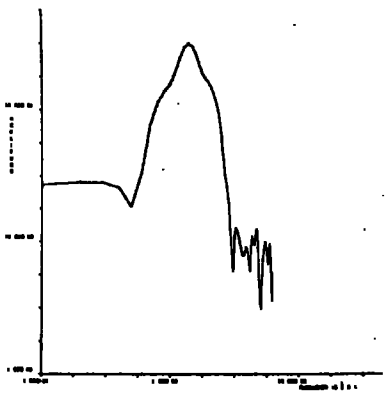

spectrum.

The general pattern of these spectra is adequately explained by Figures 18 and 19. Figure 18 shows the noise spectrum at Warramunga plotted as the total sums of the spectra at all the seismometers. [Reference - A.W.R.E. Report - A comparison of the short period seismic noise at the Four UKAEA type arrays and an estimation of their detection capabilities] The plot was obtained from analysis of thirty minute samples of background noise taken from the 1966 records. Note the minimum at 0.6 cycles per second. Figure 19 shows the seismometer response, the playout filter response and the noise spectrum superimposed on each other. The amplitude values of the three curves are arbitary. Figure 20 shows the resultant of Figure 19 alongside the amplitude spectrum at B8. From the good agreement, it is concluded that the secondary peak on all the spectra is due to microseismic noise. Any extension of a group velocity curve above 0.7 cycles per second (1.4 seconds period) and below 4 cycles per second (0.25 seconds period) must therefore be ignored.

The good agreement also suggests that the source function is an impulse with a flat frequency spectrum. This is to be expected for a mine blast.

Figure 17 shows the overall consistency of the amplitude spectra in comparison with the deviations in spectrum B1. It was mentioned in the theory that some inhomogeneity may exist under the cross-over point. Therefore a possible cause of the modulation of the B1 spectrum may be interference of reflected and refracted waves scattered from a complex structure. [Reference Pilant & Knopoff Bull. Seism. Soc. Am. Vol. 54]

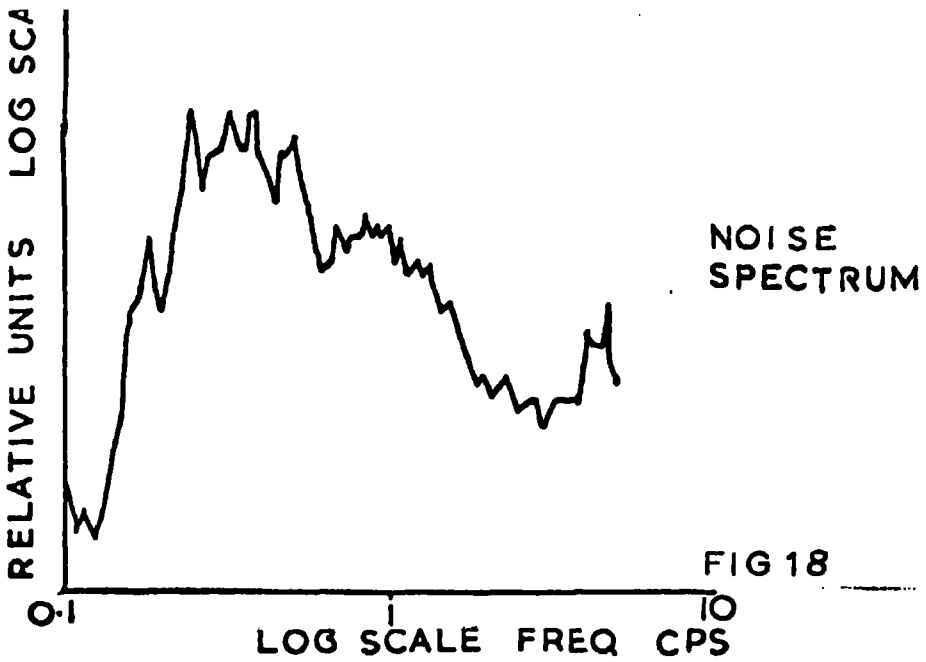

FIG 18

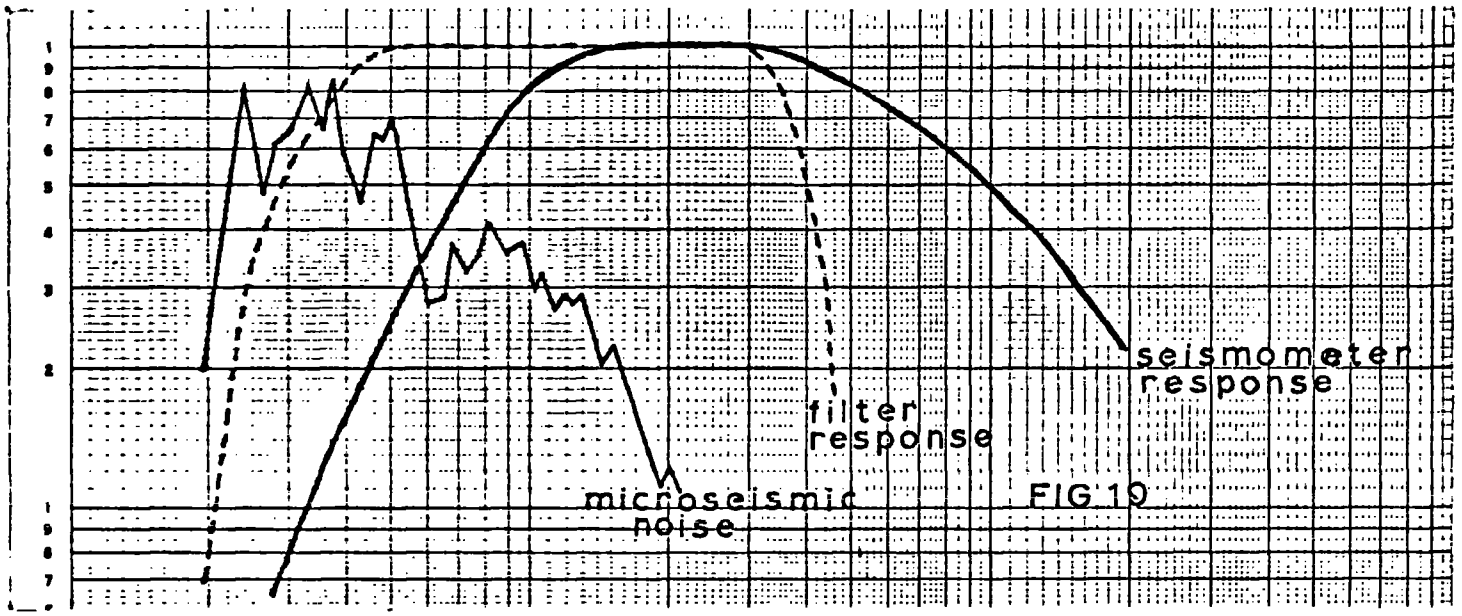

FIG 19

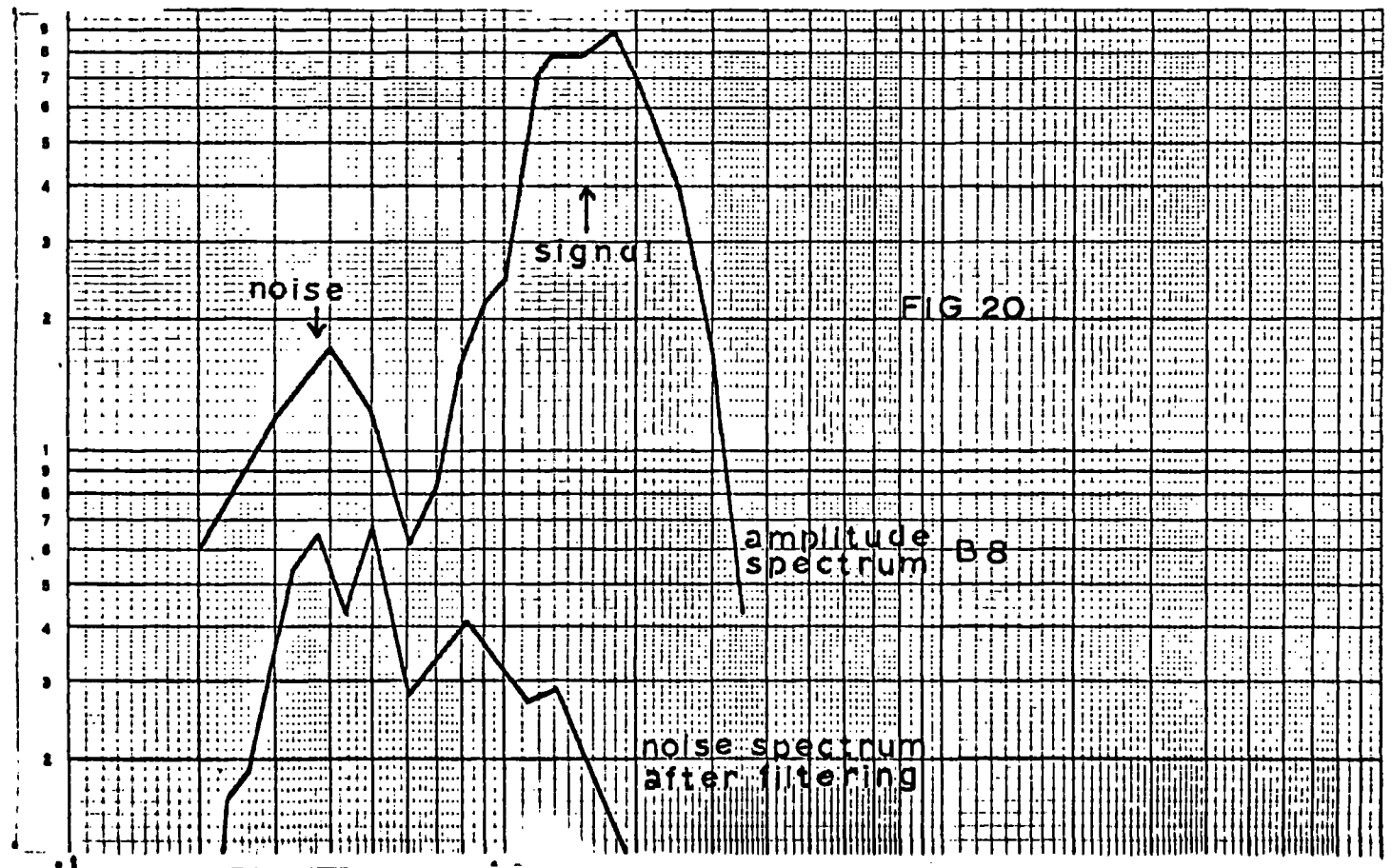

FIG 20.

GROUP VELOCITY

The output from the computer is a group velocity/period/ energy matrix. Figure 21 shows the matrix for pit B1 with relative energy contoured at 5 dB intervals. A ridge in this plot represents a dispersion curve. The plot shows that one mode is very dominant at these periods although there is some evidence of a lower mode emerging at the bottom right hand corner. Figure 22 shows the curve of the dominant ridge for two events, superimposed on the group velocity plot of Chapter Two. The trend of the group velocity curves for the two events were similar at all the pits. The difference in velocity values was attributed predominantly to the error in origin time and position. Ideally, an experiment of this type needs timed explosions.

Figures 23-26 are the group velocity curves for the arrivals at each pit. The curves could be subdivided into three general types; a positive gradient with a point of inflection at approximately 1.0 second as in B1, B3, B9, R1, R2, R6; a well developed maximum followed by a negative gradient as in B7, B8, R3 and R5; a smooth curve with one well developed minimum as in R4, R6 and R10.

It must be emphasised that the entire analysis is based on the assumption that the theory for waves in a horizontally layered medium may be assumed to apply to near surface, inevitably complex structures of dipping, undulating and possibly faulted beds. Phase changes have been shown to occur due to back scattering from a dipping interface [Knopoff and Mal; Journ. Geophys. Res. Vol. 72 pp.1769] and when a wave crosses a

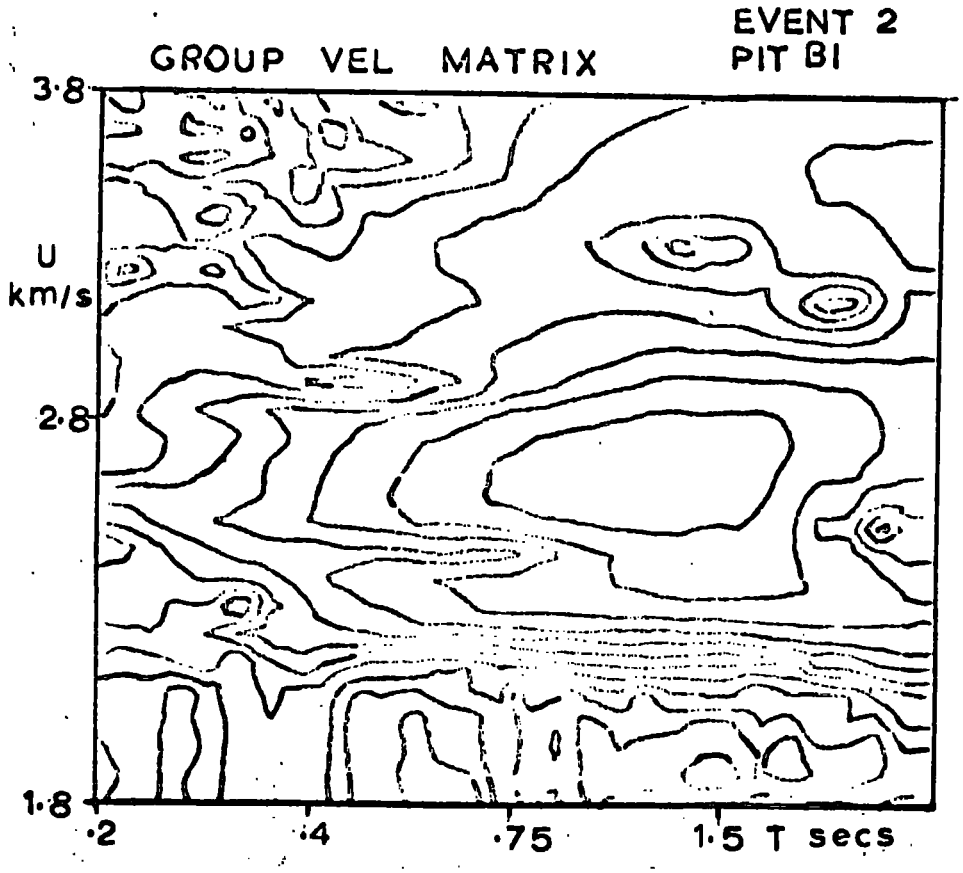
GROUP VEL MATRIX
EVENT 2
PIT B1
3·8
U
km/s
2·8
1·8
·2
·4
·75
1·5 T secs

FIG 21

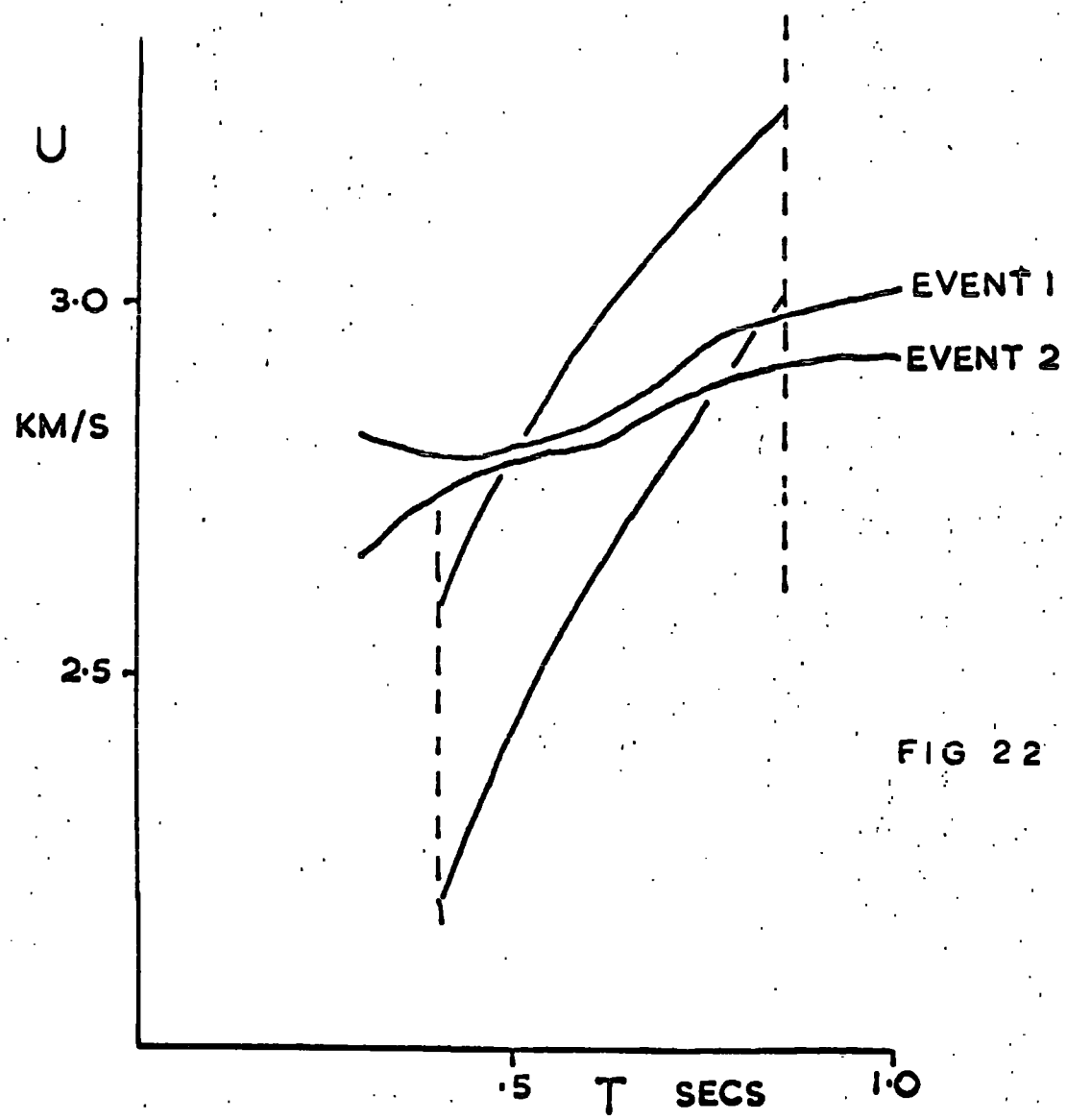
U
3·0
KM/S
2·5
EVENT 1
EVENT 2
·5
T SECS
1·0

FIG 22

FIG 23

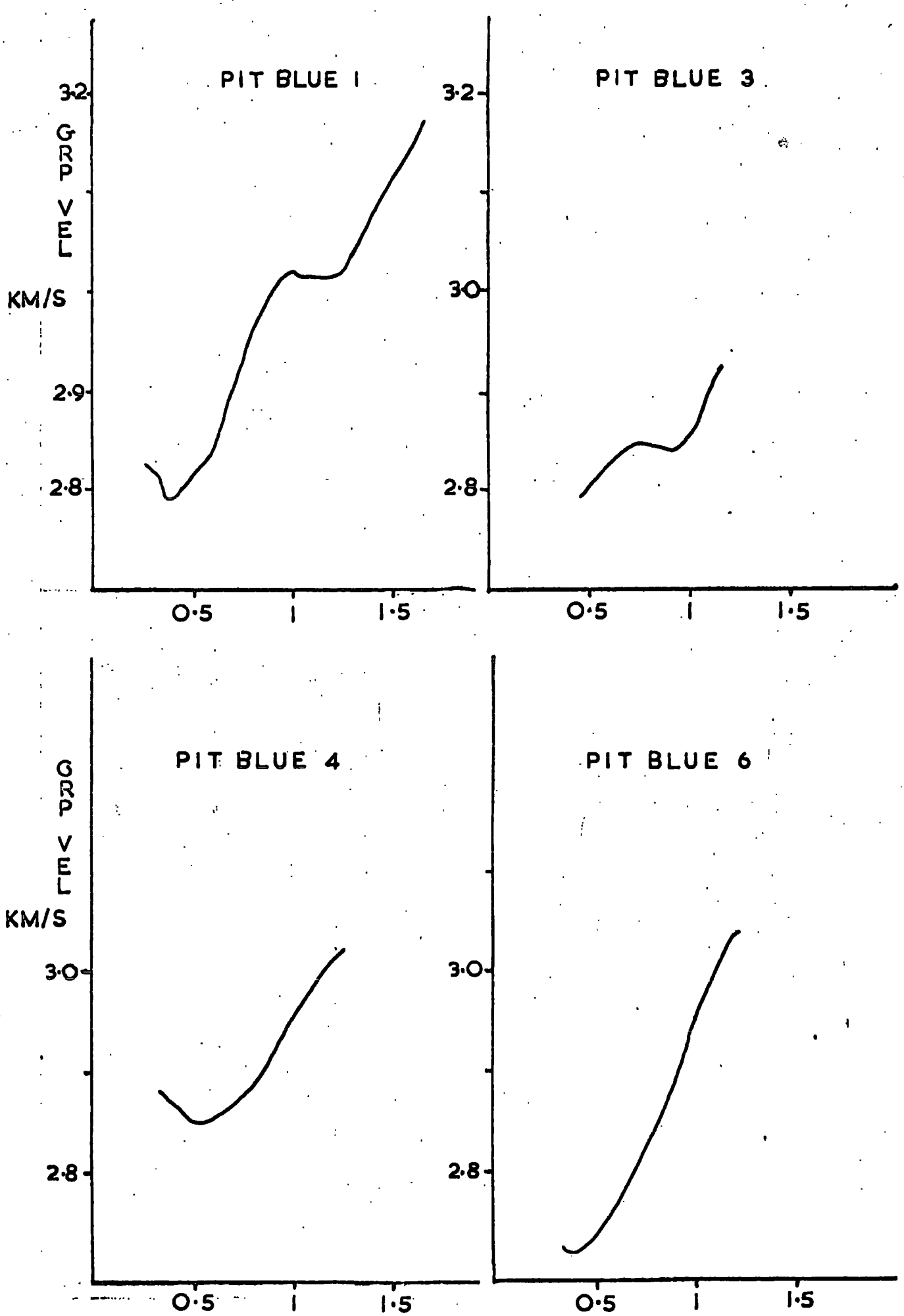
PIT BLUE 1
PIT BLUE 3
PIT BLUE 4
PIT BLUE 6
GRP VEL KM/S
3·2
3·0
2·9
2·8
0·5
1
1·5

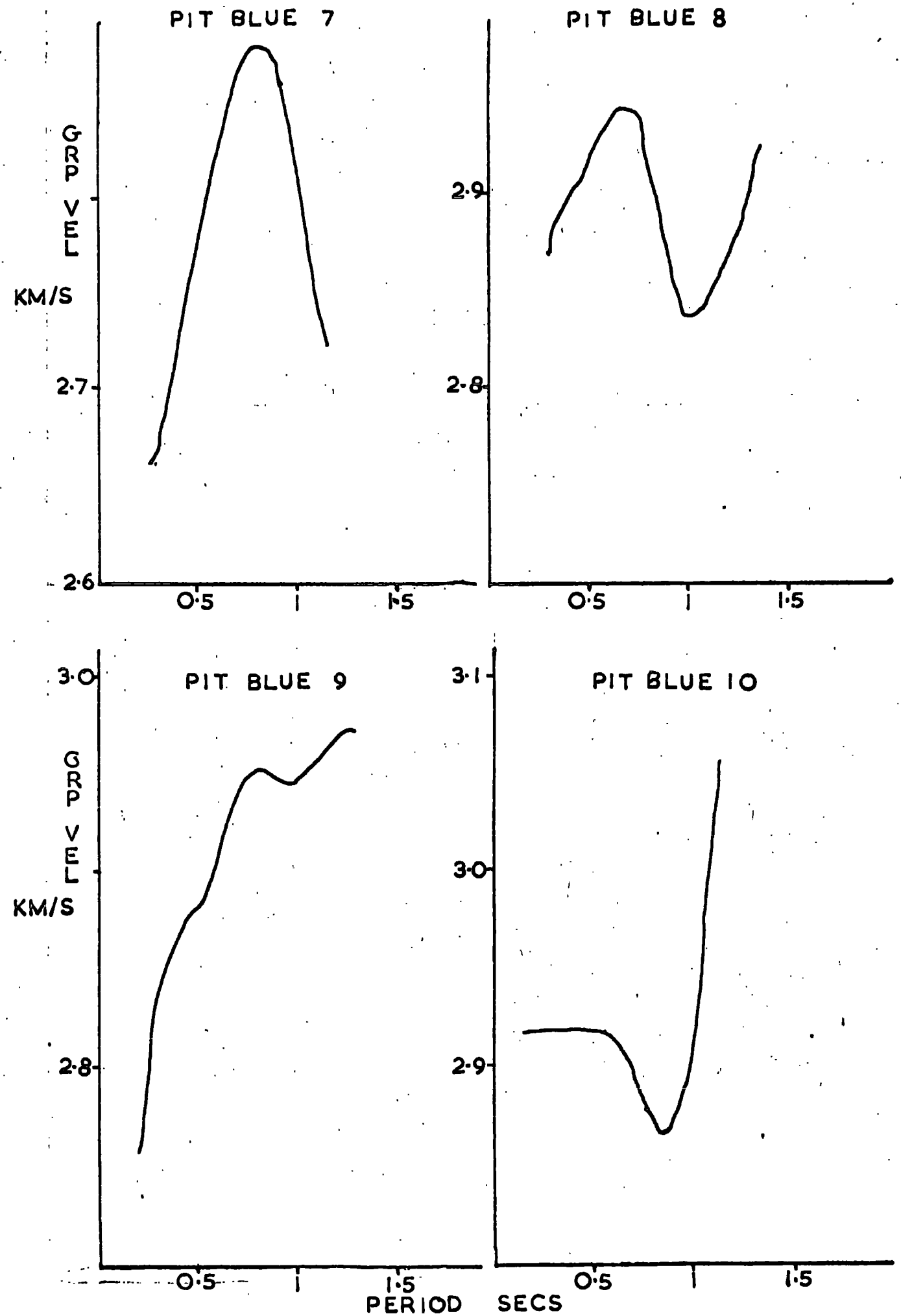
PIT BLUE 7
PIT BLUE 8
PIT BLUE 9
PIT BLUE 10
GRP VEL KM/S
2·6
2·7
2·8
2·9
3·0
3·1
0·5
1
1·5
PERIOD SECS

FIG 24

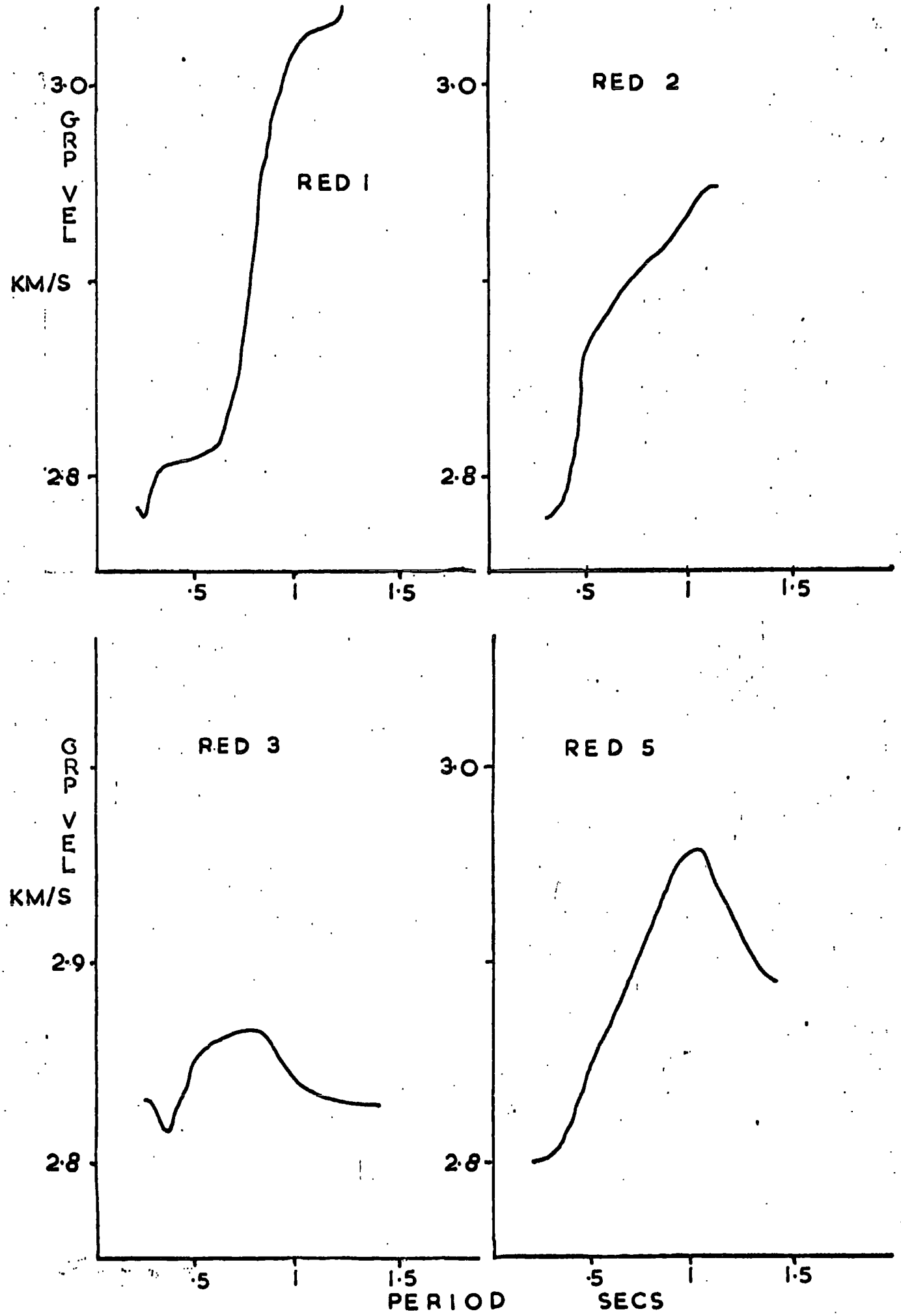

FIG 25

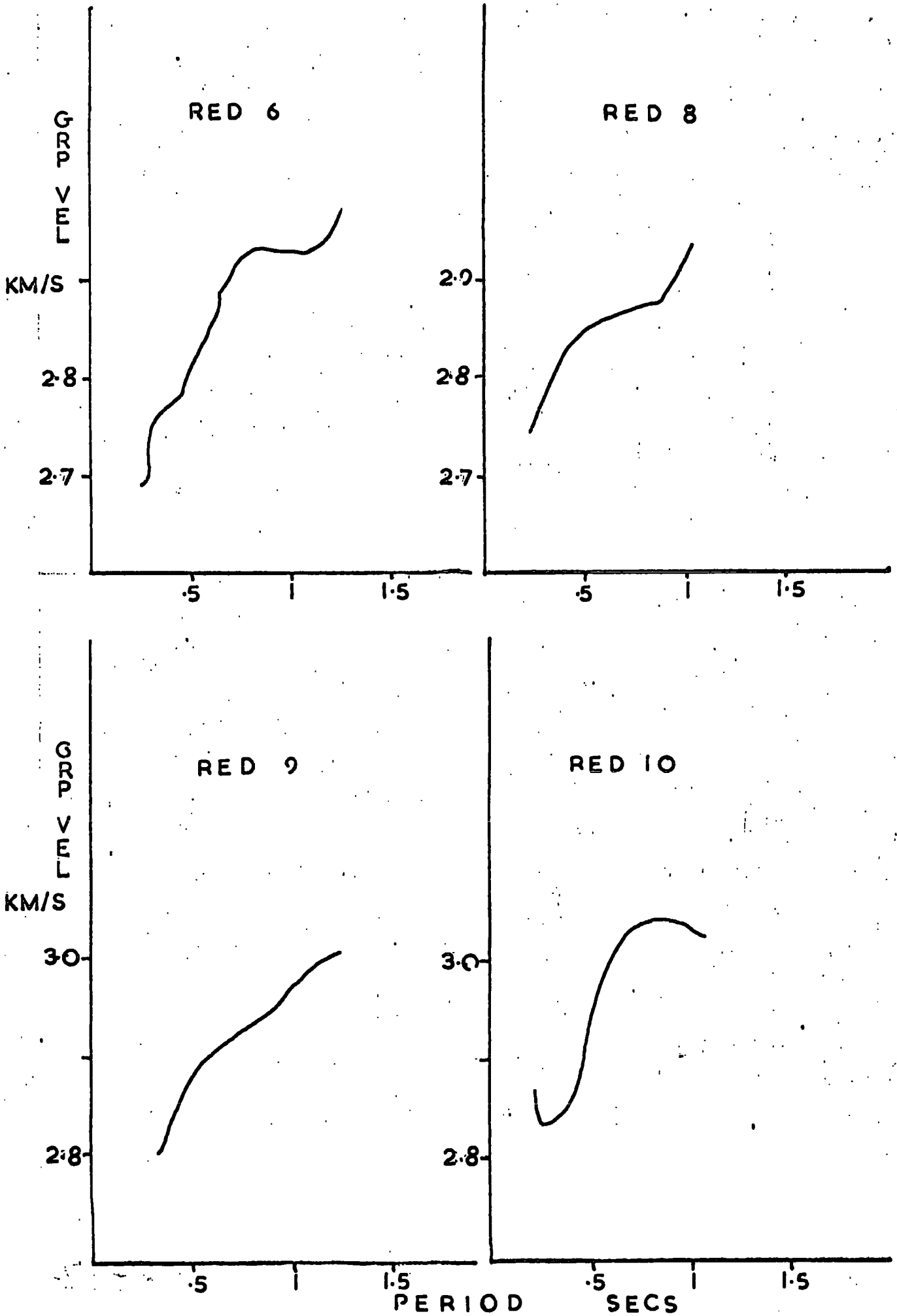

FIG 26

vertical discontinuity [Alsop; Journal Geophys. Res. Vol. 72 pp.2169]. There must be a point when approximating to a simple theory looses its validity. In this study it has been assumed that to a wave of approximately three kilometres wavelength, the structure appears to have the required simplicity.

INTERPRETATION

The following interpretation is essentially qualitative and not unique. No definite proof has been given of the mode type observed. An incorrect assumption here, would completely invalidate any conclusions. Furthermore, the error bars on the velocity values are large (see Figure 22) which limits exact quantitative analysis even if the correct mode has been chosen. However, the change in the shape of the curves across the array is significant.

A wide variety of models were fed into the Harkinder programme starting with the Underwood values. The only fundamental mode model whose theoretical curve came near to fitting the data was MODEL F. (see next sheet) See Figure 29. The inflection point has to be neglected in this interpretation. Since model F approximates to Underwood's model, this again raises the prevailing doubt about mode type. However, all other fundamental mode theoretical curves fitted very badly. They had broad minima at 1.0 seconds or above and were too slowly varying. Further analysis was therefore restricted to the first higher mode.

Having made this assumption of mode type, it was possible to suggest an explanation for the various features of the graphs. The higher mode phase velocity curve of a layer over a half space tends at its extremities to the shear velocities in the

THEORETICAL MODELS

		α km/sec	β km/sec
A			
	2.0 km	4.94	2.85
	3.0 km	5.60	3.23
		6.50	3.75
B			
	1.5 km	SAME	
	3.5 km		
C			
	2.0 km	SAME	
	4.0 km		
D			
	2.0 km	4.94	2.85
	4.0 km	5.35	3.09
		6.50	3.75
E			
	1.5 km	SAME	
	4.5 km		

All are for First Rayleigh Mode.

F			
	0.15 km	5.42	3.13
	0.75 km	5.70	3.28
		6.10	3.52

Fundamental Mode.

All densities ate 2.8 g/cc.

THEORETICAL CURVES

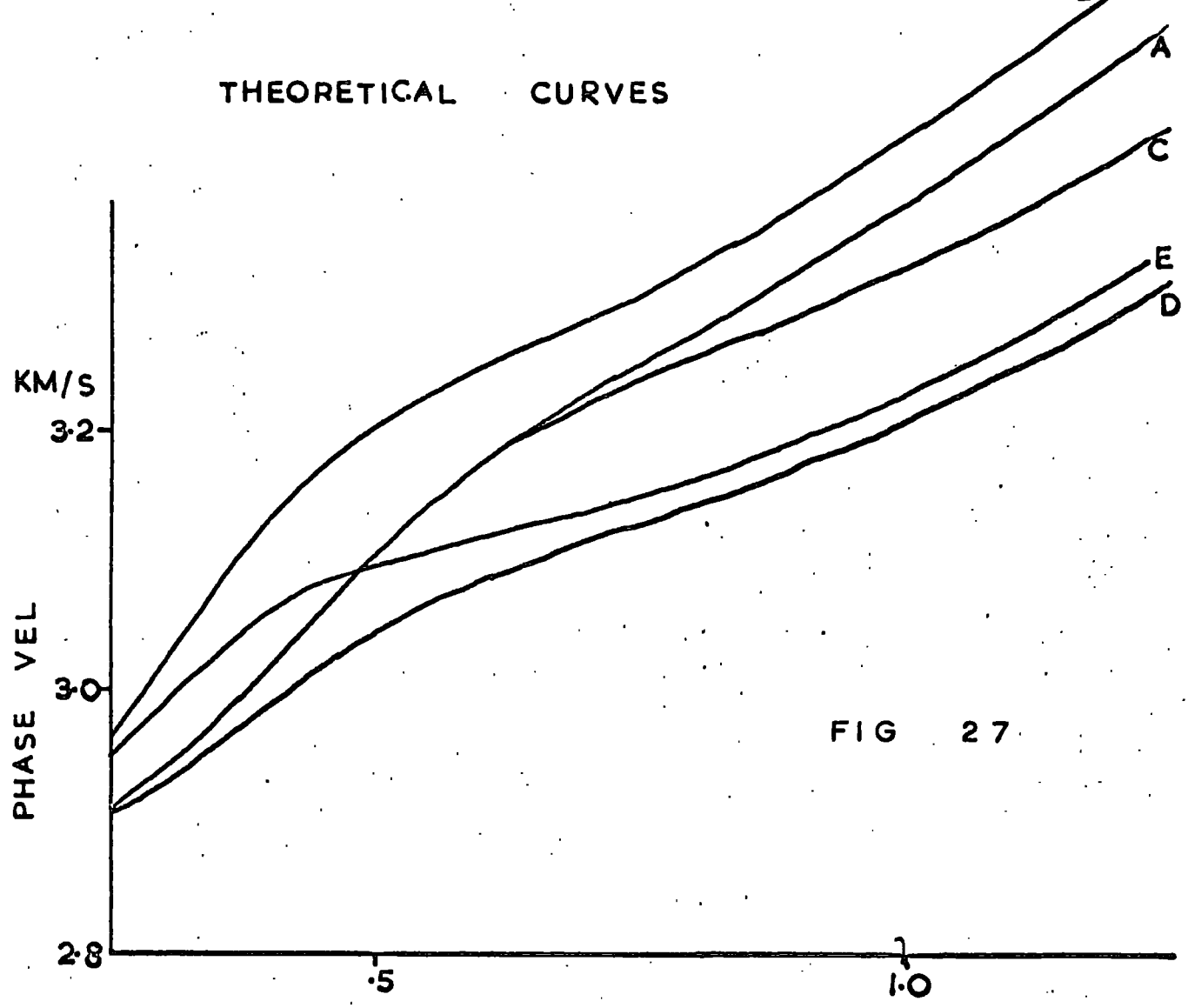

FIG 27

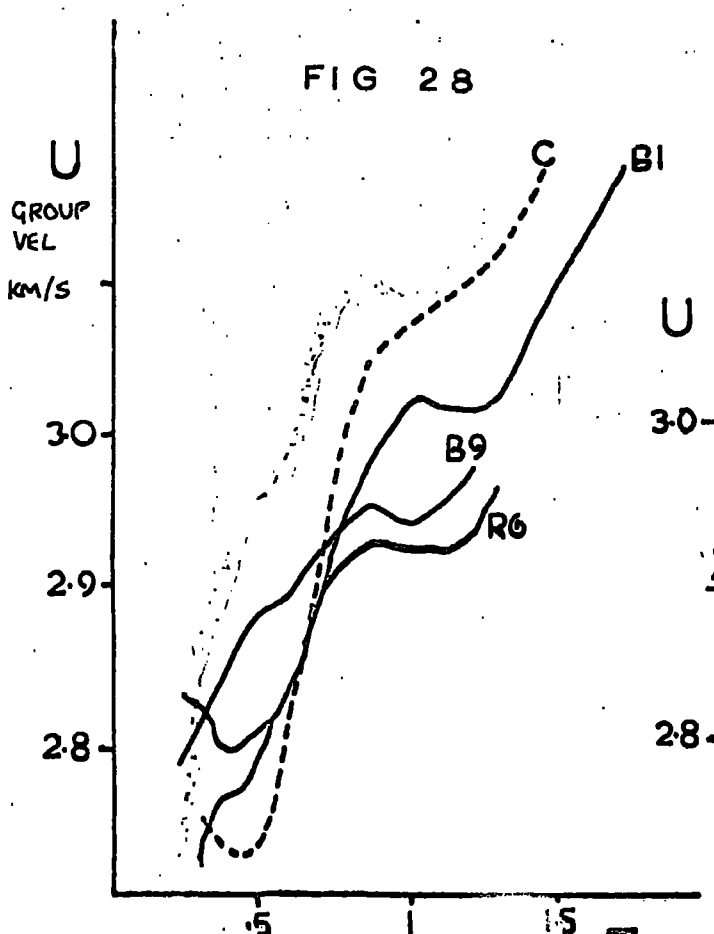

FIG 28

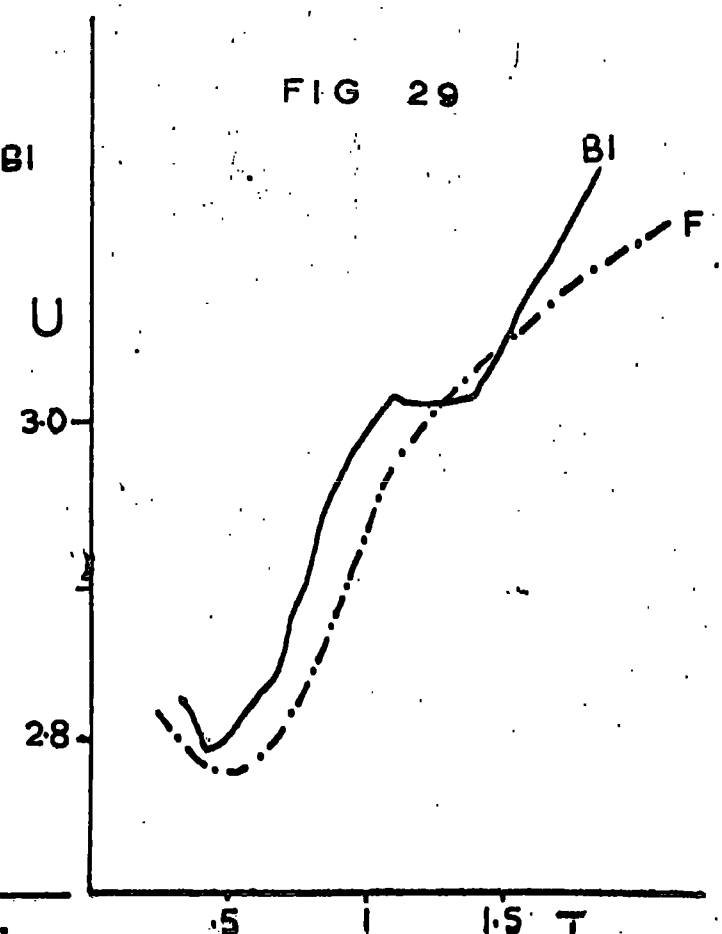

FIG 29

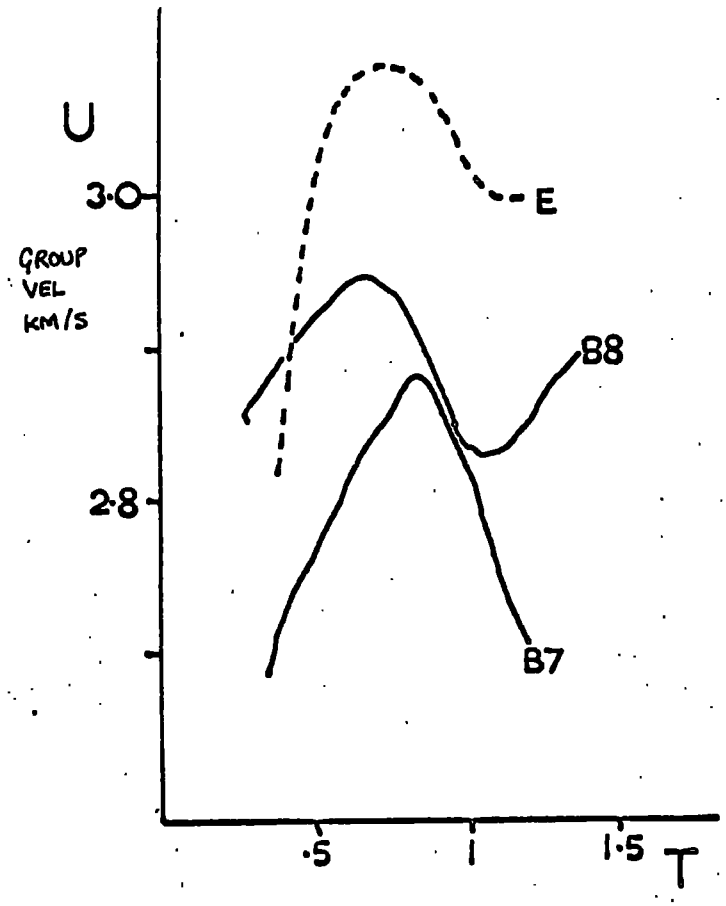

FIG 30

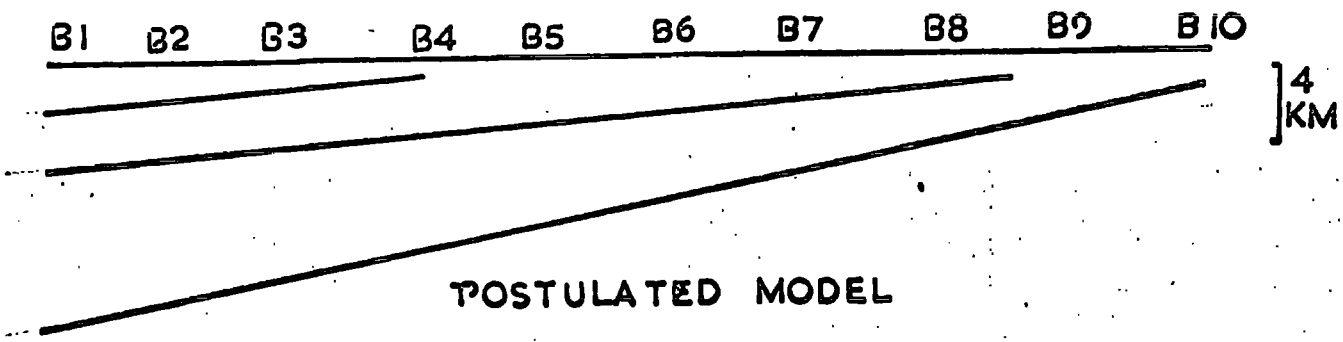

POSTULATED MODEL

FIG 31

two media. The position of maximum gradient is midway between these values. On differentiation, the resulting group velocity curve has a minimum corresponding to the maximum phase velocity gradient. In general the shape is little different for a three layer model. However, as the thickness of the middle layer increases, only the longer periods will be "aware" of the existence of a lower discontinuity. The shorter periods only propogate through a layer over a half-space. The result is a point of inflection in the phase velocity curve. [See Figure 27.] The differential of a point of inflection [i.e. the group velocity] is a maximum. For a lesser distortion in the phase velocity curve, the resultant group velocity maximum is less well developed and eventually becomes a point of inflection.

Therefore, B1, B3, B9, R1, R2, R6 and R8 are assumed to be the result of a three layer structure, B7, B8, B3 and B5 a three layer structure with a thick middle layer and B4, B6 and B10 a layer over a half space.

If this interpretation is correct, the data confirms expectations of a general structural dip towards the south-west. Figure 31 may be an approximation to the truth. Curve B9 suggests a three layer model, curve B8 and B7 a progressively deepening lower discontinuity as the maximum becomes more developed. By B6 the lower discontinuity is too deep to be detected and the structure is again effectively a layer over a half-space. B1, B3 and R1 again suggest a three layer model so the presence of a further layer is a possibility. The region of the cross-over point will be discussed again later.

Since the group velocity curve is a function of the whole

wave path from the source, the model in Figure 31 is only feasible since Peko is someway to the west of the Blue line and propogation paths vary from pit to pit.

The Red line data is similar to the Blue. If R6 to R8 reflect a three layer structure and R3 and R5 a thickening middle layer, then again one can postulate a dip towards the cross-over point as suggested by Corbishley. The three dimensional model would then have a general dip in a roughly south-westerly direction. Although this interpretation is far from unique, it is at least in broad agreement with previous work.

Figure 27 shows the variations in phase velocity brought about by relatively minor changes in the structural model. Figures 28, 29 and 30 show the fitting of theoretical curves to the data. To obtain phase velocity curves with the necessary point of inflection to produce a group velocity maximum, it was necessary to postulate a low velocity middle layer with a large velocity step at a relatively deep second discontinuity. Unfortunately Underwood's model requires a velocity of 6.10 kilometres per second at depths corresponding to the low velocity middle layer. So there is an incompatability here that is difficult to resolve.

However, the velocities of models C and E of 4.94/5.35 to 5.60/6.50 kilometres per second are again in reasonable agreement with previous work, particularly in view of the necessary horizontal layer approximation.

III,3 PHASE VELOCITY DETERMINATION BY FOURIER METHODS

Two further attempts were made to obtain phase velocity dispersion curves, since inter-pit phase velocity is dependent solely on the point at issue; the structure directly beneath the array.

Signals at a selection of pits were digitised and fourier analysed with a fast fourier computer programme, written by A. Douglas (U.K.A.E.A. Blacknest). Phase velocities were calculated from the phase spectra using standard theory, first proposed by Sâto [Bull. Earthquake Res. Inst. Tokyo Univ. 33-48 1955] for pits B1 to B3, B4 to B6, B6 to B8 and B8 to B10. The phase spectra first had to be smoothed. [Pilant and Knopoff Bull. Seism. Soc. Am. Vol. 54 1964].

Results obtained were suspect. The dispersion curves consisted of violent velocity inversions and maxima and minima which would represent the most unlikely structures. Calculations were repeated without smoothing the phase spectra, incase this had introduced undue distortion. In all cases, completely unphysical results were obtained.

It would seem that phases are too variable at these short periods for Sâto's method to be applicable. Alternatively, a wide scatter of phase velocities might result from the computation for a wave train made up of more than one mode. Smoothing might then distort the values into the sharply varying curves. In any event, the method and the results were discarded.

However, some success was obtained using a phase velocity programme written by C. Blamey and A. Douglas (U.K.A.E.A. Blacknest) and based on a method developed by Bloch and Hales [New Techniques for the Determination of Surface Wave Phase

velocities : Bull. Seism. Soc. Am. Vol. 58 No. 3, June 1968]. The output is again a matrix and Figure 32 shows the phase velocity curves at four locations with the confidence limits as the three decibell energy points along the dominant ridge.

Two features are worthy of note. Firstly, no confirmation exists for the suggestion made in Chapter Two that there is a lower near surface velocity at the north end of the blue line. Secondly, there is an apparent inversion at the cross-over point, clearly seen in B3 to R2 and to a lesser extent in B3 to B1. In a region where reflections and refractions of a surface wave occurs, an excentric dispersion curve is to be expected. Therefore, Figure 32 is possibly added confirmation of the anomalous nature of the cross-over point structure.

PHASE VELOCITY C DISPERSION CURVES

FIG 32

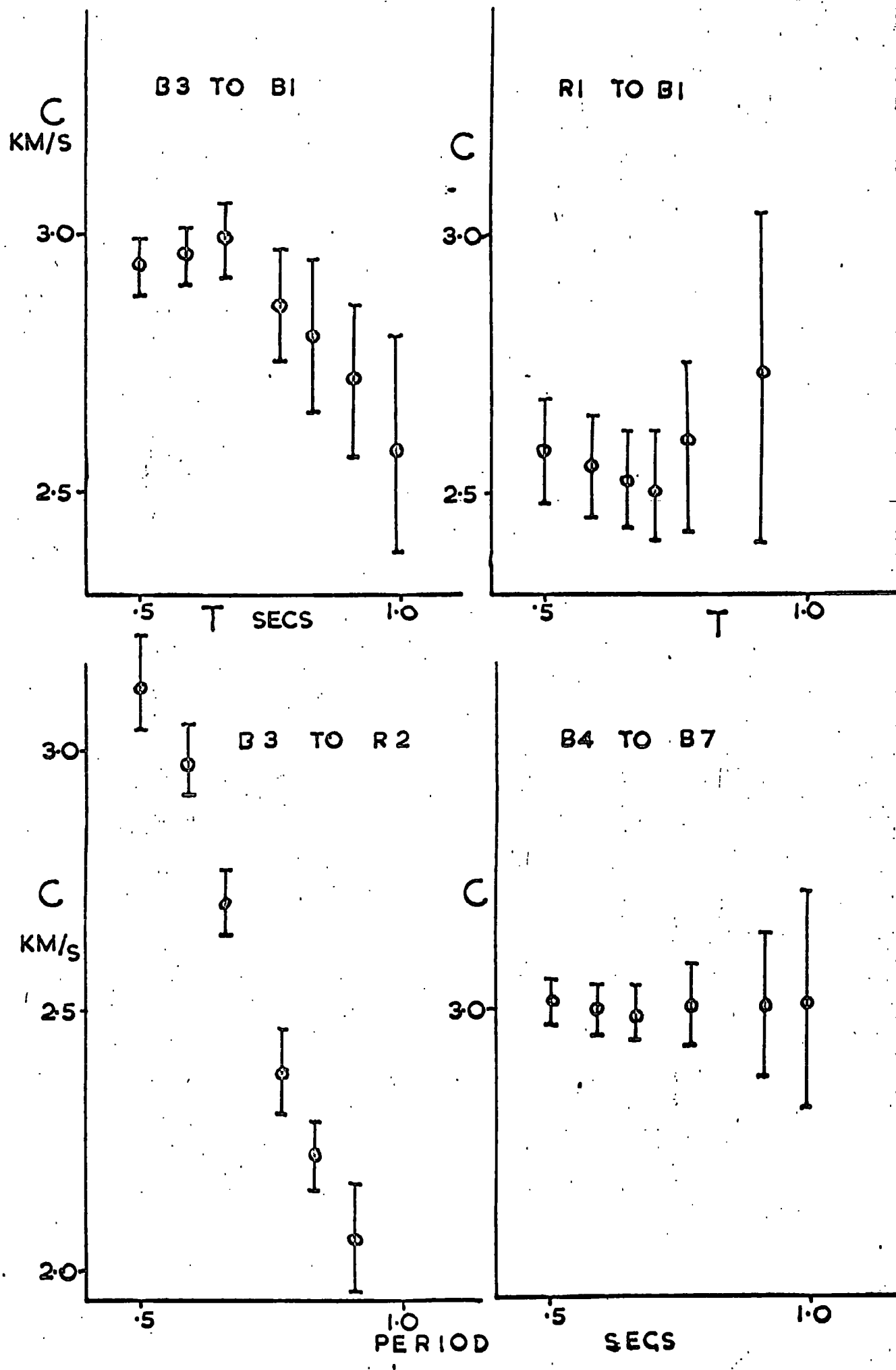

CONCLUSION

The structural model deduced from surface wave dispersion studies is in general agreement with existing models. The qualitative and approximate nature of the conclusions is not a reflection on the limitations of the analytical method. Rather it emphasises the need for a planned experiment, instead of an analysis of some vaguely convenient mine blasts. The full potentially of the method could be realised if the experiment were repeated with timed explosions located all round the array and with some three component sets of seismometers to observe particle motions and identify the mode types. Ideally, the experiment could be carried out in conjunction with a seismic reflection shoot.

In general there is no evidence to suggest that the standard techniques of dispersion analysis may not be applied to periods less than two seconds. However, the behaviour of surface waves when the structure deviates significantly from horizontal layering is little discussed in the literature but is vital to the further development of short period surface wave analysis.

APPENDIX A

HARKRIDER'S COMPUTER PROGRAMME FOR THE DETERMINATION OF THEORETICAL DISPERSION CURVES

The theoretical basis for the programme is essentially as outlined in the first part of Chapter Two. The programme sets up the matrix equation which is a function of the phase velocity, wave number and the four elastic constants of the crustal layers. An initial phase velocity and wave number value has to be specified in the data and the computer carries out an iterative proceedure, adjusting the phase velocity until the function equals zero. Then a new wave number value is specified and the process is repeated. Group velocity is obtained from the differentiation of the phase velocity curve. Having iterated onto the first root of the function, the programme, if required, will look for the next higher root, specified by the requirement that zero will be approached from the opposite sign to the first root. These results define the first higher mode. The programme only caters for a horizontal layered model.

APPENDIX B

1. SADA

The seismic array data analyser consists essentially of an analogue input, an analogue digital converter, a digital arithmetic section and a display section. Data is fed in on multi-channel F.M. magnetic tape, demodulated, filtered and equalised. The data is then multiplexed, digitised and fed directly into a core store. The read out from the core store is controlled by a programme held in a separate store. The programme calculates the delay times for each pit,

$$\tau n = -\left[\frac{xn \sin\alpha}{V} + \frac{Yn \cos\alpha}{V}\right]$$

α = azimuth, x, y = position co-ordinates of the pits

for a range of velocities and azimuths. The programme input is on punched cards.

The phased digital data is then fed to a digital adder. The partial sums of the red and blue line are cross-correlated and the result is converted back to analogue, de-multiplexed and fed into the display section. The display consists of twenty traces, corresponding to twenty different values of velocity and azimuth.

2. SADA PROGRAMME CURVED WAVE FRONT MODIFICATION

In the diagram below of the curved and plane wavefront,

$$p = r - r \cos\phi$$

The delay time correction to be applied to each seismometer is therefore,

$$\tau n = rn\ (1 - \cos\phi n) / V$$

where rn is the distance to pit n from the source,

$$\phi n = (\text{AZIMUTH data reference point} - \text{AZIMUTH n})$$

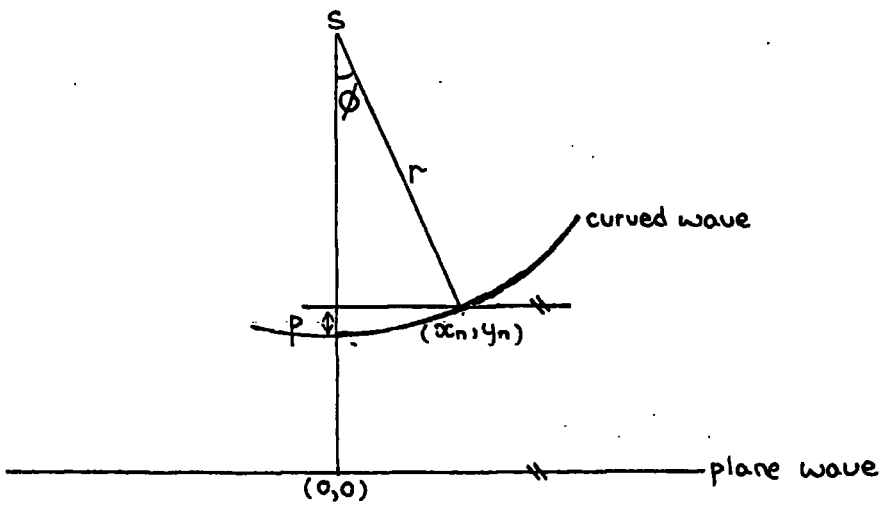

Therefore the corrected delay time is

$$\tau = -\left[\frac{xn \sin\alpha DRP}{V} + \frac{Yn \cos\alpha DRP}{V} \right] - \frac{r}{v}\left[1-\cos(\alpha DRP-\alpha n) \right]$$

CORRECTION FACTOR.

A subroutine was written that calculated the correction factor. Values of rn and αn were obtained from a programme, incorporated as an additional subroutine, which calculated the azimuths and distances between two points on the earth's surface, given the latitudes and longditudes of the points. A DO loop was then written into the main SADA programme which called up the two subroutines and provided the relevant adjustment to each delay time.

APPENDIX C

INTERPRETATION OF THE CROSS-OVER POINT MAGNETIC ANOMALY

Figure 33 shows a portion of the aeromagnetic map produced by the Bureau of Mineral Resources, Australia, in 1962. Total magnetic intensity is contoured at 50 gamma intervals. [Tennant Creek - S.E : G 237-14 June 1962] The contours are widely spaced over the rest of the array area.

The profile X-X was interpreted as resulting from a rise in a magnetic basement, using an iterative programme developed by Al-Chalabi [Durham Univ. personnal communication 1969]. The programme required no parameters to be specified other than a general initial shape and simply iterated towards a fit. The result obtained cannot be unique but does represent a plausible model.

The depth of 2.16 kilometres agrees with other work [see main text] and a similar basement rise was postulated by Cleary et al to explain anomalous cross-over point residuals. It is also interesting to note that Corbishley's dip directions at the cross-over point are directly in line with the trend of the magnetic anomaly.

CROSS-OVER POINT
MAGNETIC
INTERPRETATION

FIG 33

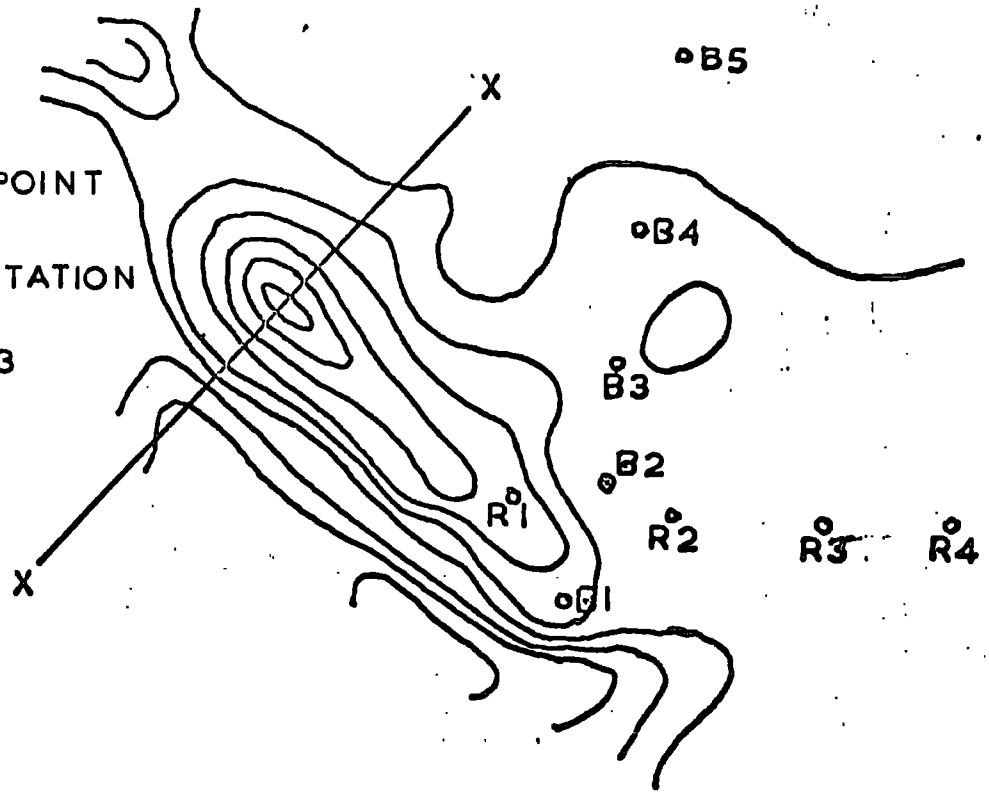

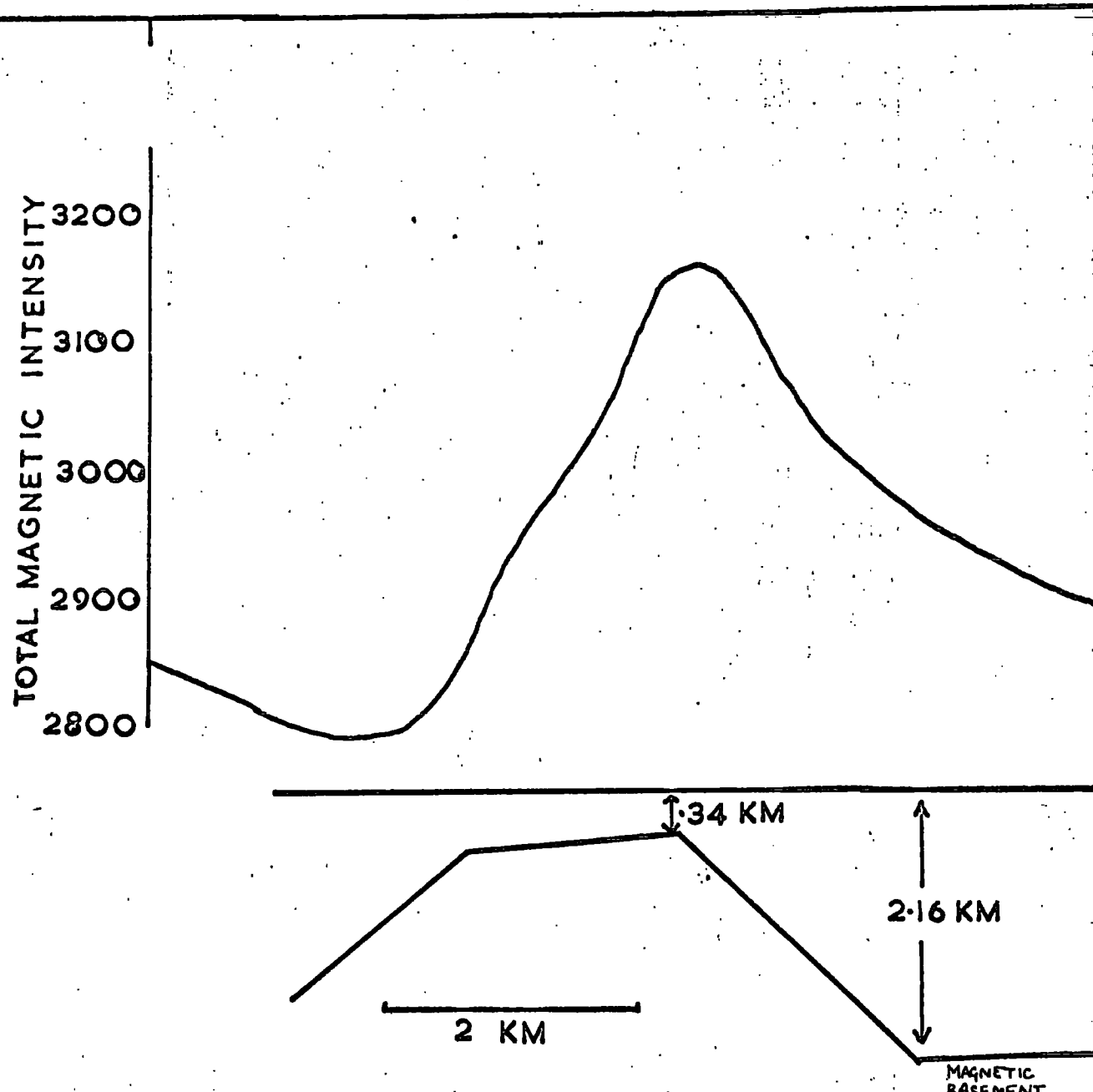

APPENDIX D

SURFACE WAVE ATTENUATION

The specific attenuation factor, Q, is the reduction to a dimensionless form of the more usual measures of attenuation. Knopoff [Revs. of Geophys. 1964 Vol. 2 No. 4] has shown that, for homogeneous material, Q may be considered to be independent of frequency. It follows that any variation of Q with frequency will be reflecting Q as a function of depth.

Tsai and Aki (Bull. Seism. Soc. Am. Vol. 59 pp.275 1969) calculated inter-station Q with surface waves of period range 15 to 50 seconds using the expression:

$$Qn = \frac{\pi f_n (r_2 - r_1)}{U} \Big/ \ln\left[\frac{A1}{A2} \sqrt{\frac{\sin \Delta 1}{\sin \Delta 2}} \right]$$

Where r_1, r_2 = distance from source to stations in kilometres

Δ_1, Δ_2 = distance from source to stations in degrees.

A_1, A_2 = Amplitude of frequency component, f_n read from the amplitude spectra.

U = group velocity at frequency f_n.

This same expression was applied to the Peko data using the amplitude and group velocity values from the group velocity programme (chapter III,2). If the amplitude spectra at these periods are too seriously modulated by surface effects or if the structure is too inhomogeneous, this simple equation completely looses its validity.

Figures 34 and 35 show the Q plots for pits B1 to B3 and B4 to B7. The values of Q are arbitary since no seismometer corrections were applied. A much more rigorous approach would

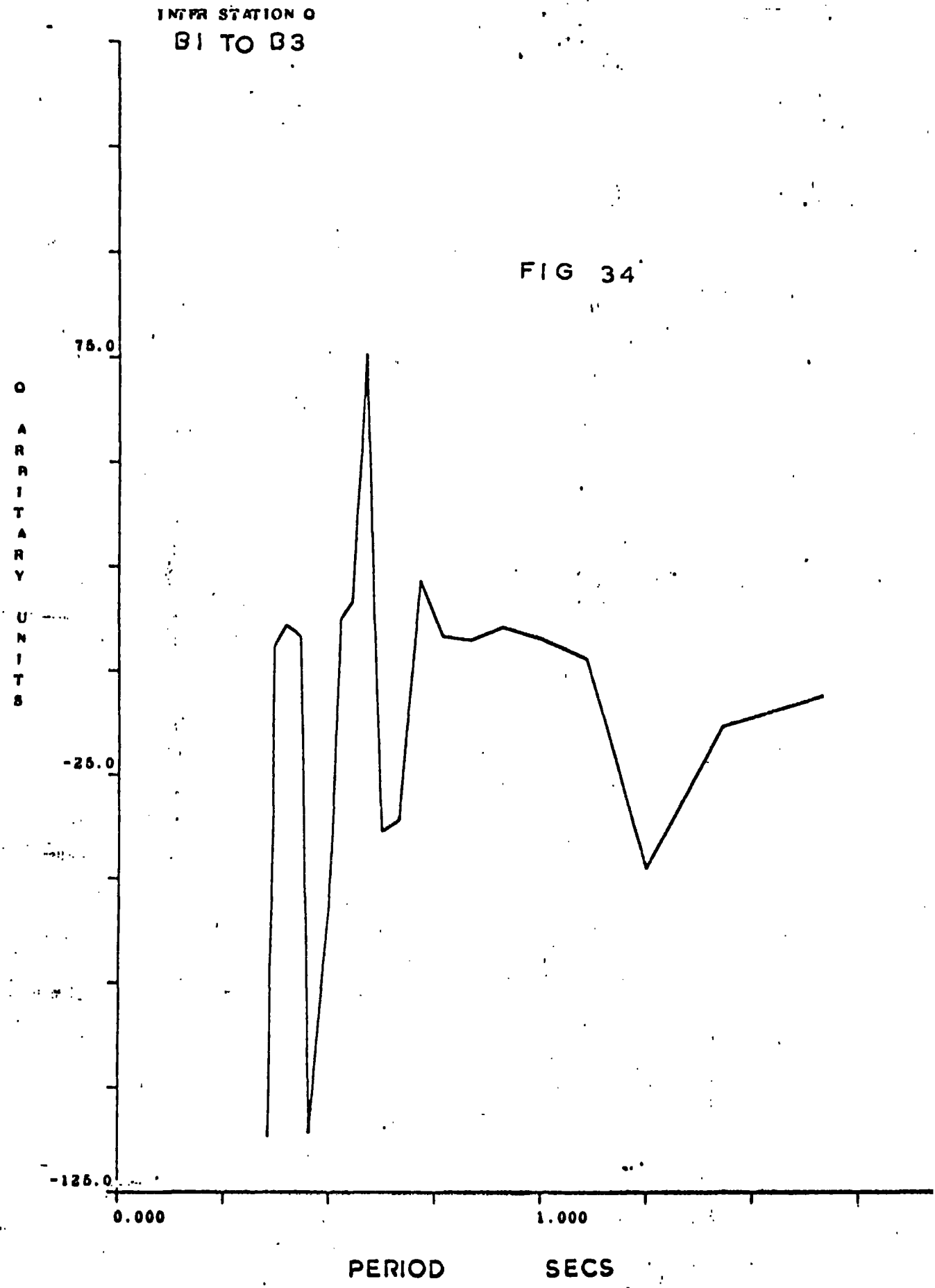
INTER STATION Q
B1 TO B3
75.0
-25.0
-125.0
Q ARBITARY UNITS
0.000
1.000
PERIOD SECS

FIG 34

INTER STATION O

B4 TO B.7

FIG 35

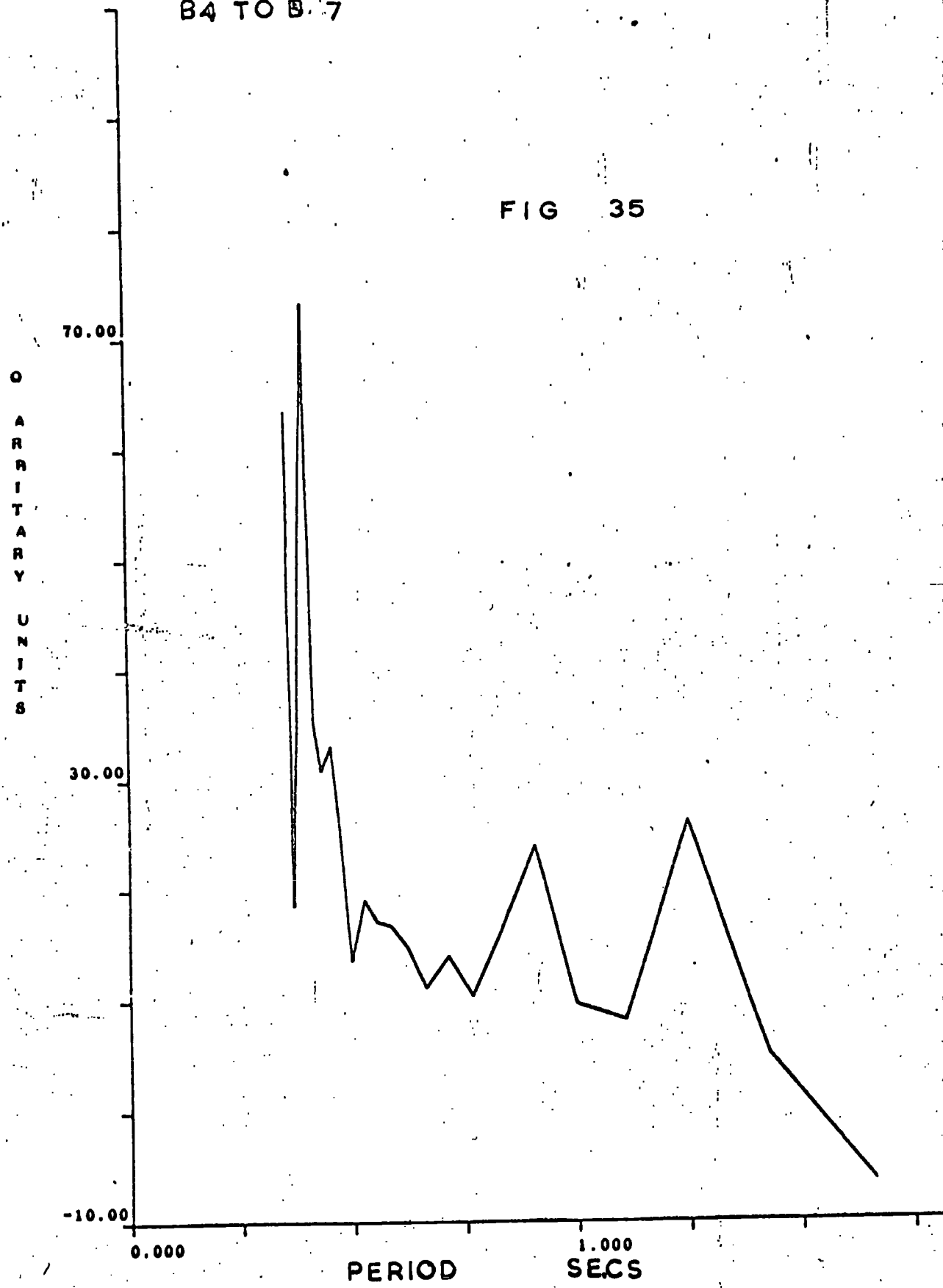

be necessary before a meaningful interpretation is possible. However, the results are encouraging. As expected, instability occurs at the short periods and the graphs have a similar minimum at 1.2 and 1.1 seconds respectively which may reflect the dipping layer postulated in Chapter III,2.

ACKNOWLEDGEMENTS

I would like to thank Dr. H. I. S. Thirlaway for allowing me to work at U.K.A.E.A. Blacknest. I am much indebted to almost every member of his staff for their constant help and advice throughout the summer, but in particular to Dr. R. Underwood for supervising me and to Mr. C. Blamey for help with his computer programmes.

In addition, my thanks are due to Dr. R. E. Long, Professor M. H. P. Bott and the Natural Enviromental Research Council.

REFERENCES

BATH M. 1968 Mathematical Aspects of Seismology. Elsevier Publishing Co.

BLOCH S. and HALES A. L. 1968 New Techniques for the determination of surface wave phase velocities. Bull. Seism. Soc. Am. Vol. 58 No. 3 pp.1021.

BRUNE J. N., NAFE J. E. and OLIVER J. E. 1960 A simplified method for the analysis and synthesis of dispersed wave trains. Jour. Geophys. Res. Vol. 65 pp.287.

BULIN N. K. and SAVARENSKY E. F. 1961 Short Period Seismic Surface Waves. I2v. Geophys. Ser. pp.855-863.

BURCH R. F. 1969 A comparison of the short period seismic noise at the UKAEA arrays. AWRE Report No. O 79/68.

CLEARY J. R., WRIGHT C. and MUIRHEAD K. J. 1968 The effects of local structure upon measurements of the travel time gradient at the Warramunga Seismic array. - in press.

CORBISHLEY D. 1969 PhD Thesis.

CRAMPIN S. 1964

(i) Higher Modes of Seismic Surface Waves: Preliminary observations. Geophys. Jour. Vol. 9.

(ii) Higher Modes: Relations to Channel Waves. Geophys. Jour. Vol. 9.

(iii) Higher Modes: Phase velocities across Scandinavia. Jour. Geophys. Res. Vol. 69 p.4801.

CROHN P. W. and OLDERSHAW W.	1965	The Geology of the Tennant Creek One-Mile Sheet Area N.T. Bureau of Min. Res. Report. No. 83.
DZIEWONSKI A., BLOCH S. and LANDISMANN M.	1969	A technique for the analysis of transient seismic signals. Bull. Seism. Soc. Am. Vol.59 p.427.
EWING W., JARDETZKY W., and PRESS F.	1957	Elastic Waves in Layered Media. McGraw-Hill.
GLOVER P. and ALEXANDER S. S.	1969	Lateral Variations in crustal structure under LASA. Jour. Geophys. Res. Vol. 74 p.505.
HASKELL N. A.	1953	The dispersion of surface waves in multi-layered media. Bull. Seism. Soc. Am. Vol. 43 p.17.
HERRMANN R. B.	1969	The structure of the Cincinnati Arch as determined by Short period Rayleigh waves. Bull. Seism. Soc. Am. Vol. 59 p.399.
KNOPOFF L.	1964	'Q'. Rev. Geophys. Vol. 2 No. 4.
KNOPOFF L. and MAL	1967	Phase Velocity of surface waves in the transition zone of continental margins. Jour. Geophys. Res. Vol. 72 p.1769.
LINVILLE A. F. and LASTER S. J.	1967	Near Surface Dispersion Studies at Tonto Forest Seismic Obs. Bull. Seism. Soc. Am. Vol. 57 p.311.
McEVILLY A. F. and STAVDER S. J.	1965	Effect of Sedimentary thickness on Short-Period Rayleigh wave dispersion. Geophys. Vol. 30 No. 2.
McGARR A. and ALSOP L. F.	1967	Rayleigh wave transmissions and reflections. Jour. Geophys. Res. Vol. 72 p.2169.

MOONEY H. M. and BOLT B. A.	1966	Dispersive Characteristics of the first three Rayleigh Modes of a simple surface layer. Bull. Seism. Soc. Am. Vol. 56 p.43.
OLIVER J. and EWING M.	1958	The effect of Surficial Sedimentary Layers on Continental Surface Waves. Bull. Seism. Soc. Am. Vol. 48 p.339.
PILANT W. L. and KNOPOFF L.	1964	Observations of Multiple Seismic Events. Bull. Seism. Soc. Am. Vol. 54 p.19.
PRESS F., HARKRIDER D. and SEAFELDF C. A.	1961	A fast convenient programme for computation of surface wave dispersion curves in multi-layered media. Bull. Seism. Soc. Am. Vol. 51 p.495.
SÂTO	1955	Analysis of Dispersed Surface Waves by Fourier Transform. Bull. Earthquake Res. Inst. Rokyo Univ. 33-48.
TSAI, YI-BEN and AKI K.	1969	Simultaneous Determination of the seismic moment and attenuation of seismic surface waves. Bull. Seism. Soc. Am. Vol. 59 p.275.
UNDERWOOD R.	1968	The structure under the Warramunga seismic array near Tennant Creek, Australia. Royal Astronom. Soc. March 1968